CRISPR-Cas9-Based Genetic Modification of the Industrially Useful Fungus *Aspergillus terreus*

Logan Robeck

A Thesis
in
The Department
of
Chemistry and Biochemistry

Presented in Partial Fulfillment of the Requirements
for the Degree of Master of Science (Chemistry) at
Concordia University
Montreal, Quebec, Canada

October 2019

CONCORDIA UNIVERSITY

School of Graduate Studies

This is to certify that the thesis prepared

By: Logan Robeck

Entitled: CRISPR-Cas9-Based Genetic Modification of the Industrially Useful Fungus *Aspergillus terreus*

and submitted in partial fulfillment of the requirements for the degree of

Master of Science (Chemistry)

complies with the regulations of the University and meets the accepted standards with respect to originality and quality.

Signed by the final Examining Committee:

_____ Chair

Jung Kwon Oh

_____ Examiner

Brandon Findlay

_____ Examiner

Adrian Tsang

_____ Supervisor

Justin Powlowski

Approved by _____

Yves Gélinas

_____ 2019 _____

Andre Roy

ABSTRACT

CRISPR-Cas9-Based Genetic Modification of the Industrially Useful Fungus *Aspergillus terreus*

Logan Robeck

In recent years there has been increased interest in the production of valuable materials through the use of microbes to convert biomass[1]. The filamentous fungus *Aspergillus terreus* is already of industrial value through its ability to produce the cholesterol lowering drug lovastatin, and the bulk commodity chemical itaconic acid [2]. While itaconic acid already has a market of up to 80,000 tons per year, it can also be used as a replacement for the petrochemical derived acrylic acid, which has a market of 2,100,000 tons, for several applications[3]. However, additional research is needed to improve production of itaconic acid using *A. terreus* to lower its production cost to make it more competitive against acrylic acid. Unfortunately, research into itaconic acid production has been hampered by shortcomings in genetic manipulations of *A. terreus*[3]. Here, is described the first use of CRISPR-Cas9-based genetic modifications as a means of producing new strains of *A. terreus* for future study. This study describes the creation of stable strains with genetic changes, opening the door for future investigations into *A. terreus* that may improve itaconic acid production.

Acknowledgments

My sincere thanks to Dr. Powlowski and Dr. Tsang for their patience and mentorship throughout this long process. My time working with the two have you has been one of immense growth for which I am very grateful. I'd also like to thank my coworkers for their constant support and encouragement. Among these I especially owe Dr. Pham and Dr. Ouedraogo who I haunted for years in my constant pursuit for clarification and information. My friends and family also deserve a great deal of credit, without their support I would not have been able to weather the stress of the last few years.

Special acknowledgements go to Sandrine Marqueteau for the extraction of the sequenced *Aspergillus terreus* DNA, to Debra Fulton for constructing the scaffold assembly, and to Alexandre Beaudoin for compiling it in BLAST server.

Funding was generously provided by NSERC, the Industrial Biocatalysis Network, Concordia University, and the Garnet Strong Scholarship.

Table of Contents

List of Figures

List of Tables

List of Abbreviations

5-FOA	5-Fluoroorotic Acid
CM	Complete Media
CRISPR	Clustered Regularly Interspaced Palindromic Repeats
GRAS	Generally Recognized As Safe
MEA	Malt Extract Agar
NSRM	Non-Selective Regeneration Media
OM	Osmotic Media
PEG	Polyethylene Glycol
SRM	Selective Regeneration Media
STC	Sucrose Tris Calcium Chloride Buffer
TB	Tris Buffer
TC	Tris Calcium Chloride Buffe

Introduction

In recent years widespread use of petrochemicals has been subjected to increased scrutiny due to concerns about environmental impact and sustainability. However, several industries are still wholly or majorly dependent upon petrochemicals. One such example is the polymer industry wherein the diverse range of readily available and cheap chemicals derived from fossil fuels are the primary feedstocks for a range of ubiquitous products such as plastics, resins, epoxies, and coatings. The combination of increased concerns over fossil fuel consumption and continued demand for their products has led to interest in the development of platform chemicals from renewable resources[4].

One such chemical is itaconic acid (2-methylene succinic acid, Figure 1), which is readily produced from carbohydrates by the submerged fermentation of the microorganism *Aspergillus terreus*[5]. Itaconic acid can be used instead of the related compound, acrylic acid (Figure 1), which is produced from fossil fuels, for a variety of industrially valuable reactions[6]. Unfortunately, the current market for itaconic acid is limited by the fact that acrylic acid remains cheaper than itaconic acid despite decades of investigations into the improvement of biotechnological itaconic acid production. As a result there exists a need to further optimize the production of itaconic acid to increase its economic viability as a renewable alternative to acrylic acid [7].

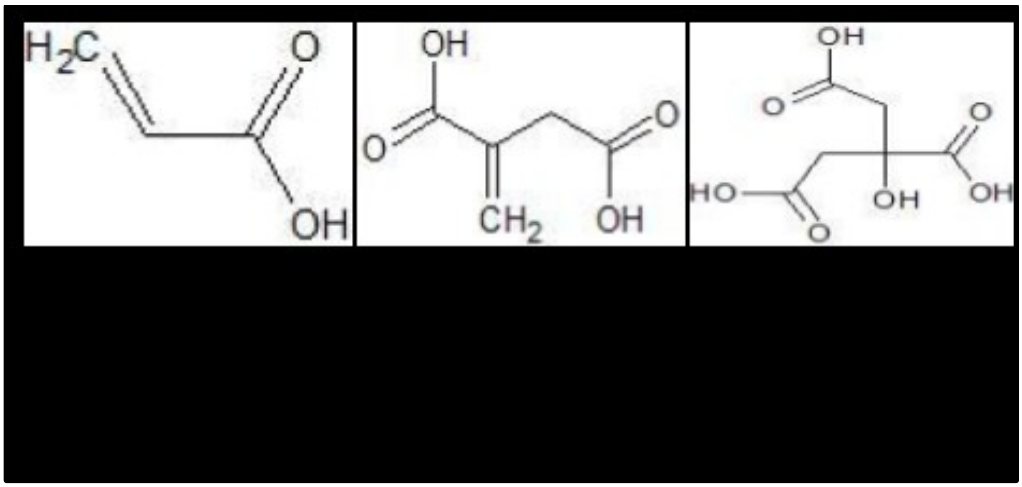

Direct process development such as the optimization of media components or growth conditions has been widely and extensively investigated for the production of itaconic acid [8–10]. Genomics-based approaches are also possible but require that the appropriate tools are in place for the manipulation of the fungal host. Here, the focus is on the application of CRISPR-Cas9 to the production of strains of *A. terreus* for construction of genome knockouts intended ultimately for the improvement of itaconic acid production.

Production of Acrylic and Itaconic Acids

Acrylic acid is a small 3-carbon compound consisting of a vinyl group attached to a carboxyl group (Figure 1). Due to its two reactive groups it readily polymerizes either with itself or other monomers, leading to a vast range of products such as plastics, coatings, epoxies, resins, and various other materials collectively known as “acrylics”. It is manufactured industrially from the oxidation of propylene or propane, derived from crude oil [11]. Currently over 5 million tons of acrylic acid are consumed worldwide with market projections expecting demand to increase to around 8 million tons by 2020 [4]. As a result, the production and use of acrylic acid represent a huge source of carbon release and will continue to do so for decades to come unless changes are made to consumption, production, or use of more sustainable alternatives.

While the simplicity, functionality, and low cost of acrylic acid make it an ideal platform chemical, compounds with similar properties are well known and readily available. One such compound is the currently more expensive, but more sustainably produced, itaconic acid (Figure 1). Itaconic acid is a mono-unsaturated dicarboxylic acid that at room temperature is a white crystalline solid with the chemical structure and properties shown in Table 1. It was discovered in 1837 by S. Baup who produced it as a thermal decomposition product of citric acid (Figure 1)[12]. This became one of the early means of chemical production with the first synthesis being performed shortly thereafter by Crasso (cited by Cordes et al. 2015 [13]).

Table 1: Properties of Itaconic Acid and Citric Acid

	Itaconic Acid	Citric Acid
Chemical Formula	$C_5H_6O_4$ [6]	$C_6H_8O_7$ [14]
Molecular Weight	130.1 g/mol [6]	192.12 g/mol [14]
pK_a Values	3.84 and 5.55 [6]	3.13, 4.76, and 6.39 [14]
Solubility in H_2O at 20°C	83 g/L [6]	147.76 g/100 mL[14]
Theoretical Max Yield ($g_{acid}/g_{glucose}$)	0.72 g/g [3]	1.06 g/g [3]
Price Per Kilogram	USD $1.80-2.00 [6]	USD $0.68 [15]
Total Estimated Market (tons)	41,000-80,000 [3]	2,100,000 [3]

The potential of itaconic acid as a replacement for acrylic acid is all the more attractive given the fact that unlike the vast majority of currently utilized platform chemicals, itaconic acid can be produced biologically. Initially it was reported in

Aspergillus itaconicus[16], and then later found to be produced by *Aspergillus terreus* with higher yields [17]. It was for a process using submerged fermentation of *Aspergillus terreus* that Charles Pfizer Co. applied for a patent in 1945, leading to the first production plant in 1955. Since this point, biotechnological generation of itaconic acid using *A. terreus* has been dominant over chemical synthesis as the means of industrial production [6].

The presence of functionally active sites on the molecule (the two carboxyl groups and the methylene group) make itaconic acid a useful starting material for a variety of reactions and products. Of primary industrial interest are polymerization reactions wherein itaconic acid is an effective substitute for the fossil fuel derived acrylic acid and related compounds [18]. Unfortunately, the price of itaconic acid still surpasses that of acrylic acid, and this has limited the adoption of itaconic acid as an alternative feedstock for many of the processes now involving acrylic acid, and as a platform chemical for its own separate processes [3,5].

Numerous studies have focused on cost effective ways of improving the final titer and yield of itaconic acid by *A. terreus* so that it can more effectively compete with the price of acrylic acid. This focus was further sharpened by the inclusion in 2004 of itaconic acid in the US Department of Energy's list of "Top Value Added Chemicals from Biomass" [1]leading to increased interest, with several research publications mentioning this release [8,19,20]. Indeed, itaconic acid already has a substantial market estimated to be around 41,000 tons with future predictions of a dramatic increases in demand of anywhere from 80,000 to more than 400,000 tons by 2020, depending on how effectively itaconic acid can compete with other building block compounds such as methacrylic and polyacrylic acids [3,21,22].

Properties of *A. terreus*

A. terreus is a ubiquitous saprophytic filamentous fungus. It is found in soil globally with especially high prevalence in tropical and subtropical climates [23]. It

produces a characteristic yellow pigment, and mature cultures exhibit light to dark brown spores [24]. Originally described by Thom and Church[25], who were themselves quoting the works of Wehmer, it has a long history of interactions with humans. In addition to its industrial use in the production of itaconic acid it also has a history of use in the production of valuable enzymes such as xylanases [26]. Interestingly, *A. terreus* was the original source of lovastatin, one of the first in the line of widely used cholesterol lowering drugs known as statins, which accounted for a 4-5 billion dollar industry in 2012 [26,27]. While biotechnological production of lovastatin has largely been replaced by chemical synthesis of later generation statins, the continued dominance of biotechnological production of itaconic acid over chemical synthesis and the predicted increases in demand for itaconic acid suggest a continued utilization of *A. terreus* for years to come [3]. As is expected, itaconic acid's development as a commodity chemical initiated a desire to better understand the specifics of its *in vivo* production in *A. terreus.*

Biochemistry of Itaconic Acid Production by *A. terreus*

While the metabolic pathway that leads to the production of itaconic acid in *A. terreus* is still a matter of some debate, the generally accepted route (Figure 2A[6]) is that the sugar feedstock is introduced into glycolysis and the pentose phosphate pathway in the cytosol where it is converted into pyruvate. The resultant pyruvate is then transported into mitochondria and introduced into the Tri-Carboxylic Acid Cycle (TCA Cycle) where it is converted into *cis*-aconitate. *Cis*-aconitate is then transported back into the cytosol via a transporter that has tentatively been identified as either a mitochondrial tricarboxylate transporter or a citrate-malate antiporter MttA (MttA transporter)[4]. Once returned to the cytosol *cis*-aconitate is decarboxylated by the enzyme *cis*-aconitate decarboxylase (CadA) thus yielding the final product, itaconate, which is hypothesized to be secreted into the media via a major facilitator superfamily (MfsA) transporter [3,7].

The "itaconic acid cluster" (Figure 2B) is usually described as comprising these three genes, mitochondrial tricarboxylate transporter, major facilitator superfamily transporter, and *cis*-aconitate decarboxylase (*mttA*, *mfsA*, and *cadA*), together with a

nearby Zn_2Cys_6-transcriptional regulator, which are clustered in the genome of *A. terreus* [6]. Sometimes the upstream TCA cycle genes (citrate synthase and isocitrate dehydrogenase) are also considered to be part of the cluster [3,28]. However no direct evidence has been reported for the transcription factor's role in itaconic acid synthesis, thus the regulation of this process is still a mystery [20]. A complicating factor is this pathway's close association with the TCA cycle, a central pathway of metabolism. This association is likely a factor in the high yields of itaconic acid that can be observed, however it also limits the potential to investigate itaconic acid's production via

mutational analysis as the genes upstream of itaconic acid biosynthesis are all TCA cycle genes and are therefore necessary for the organism's survival.

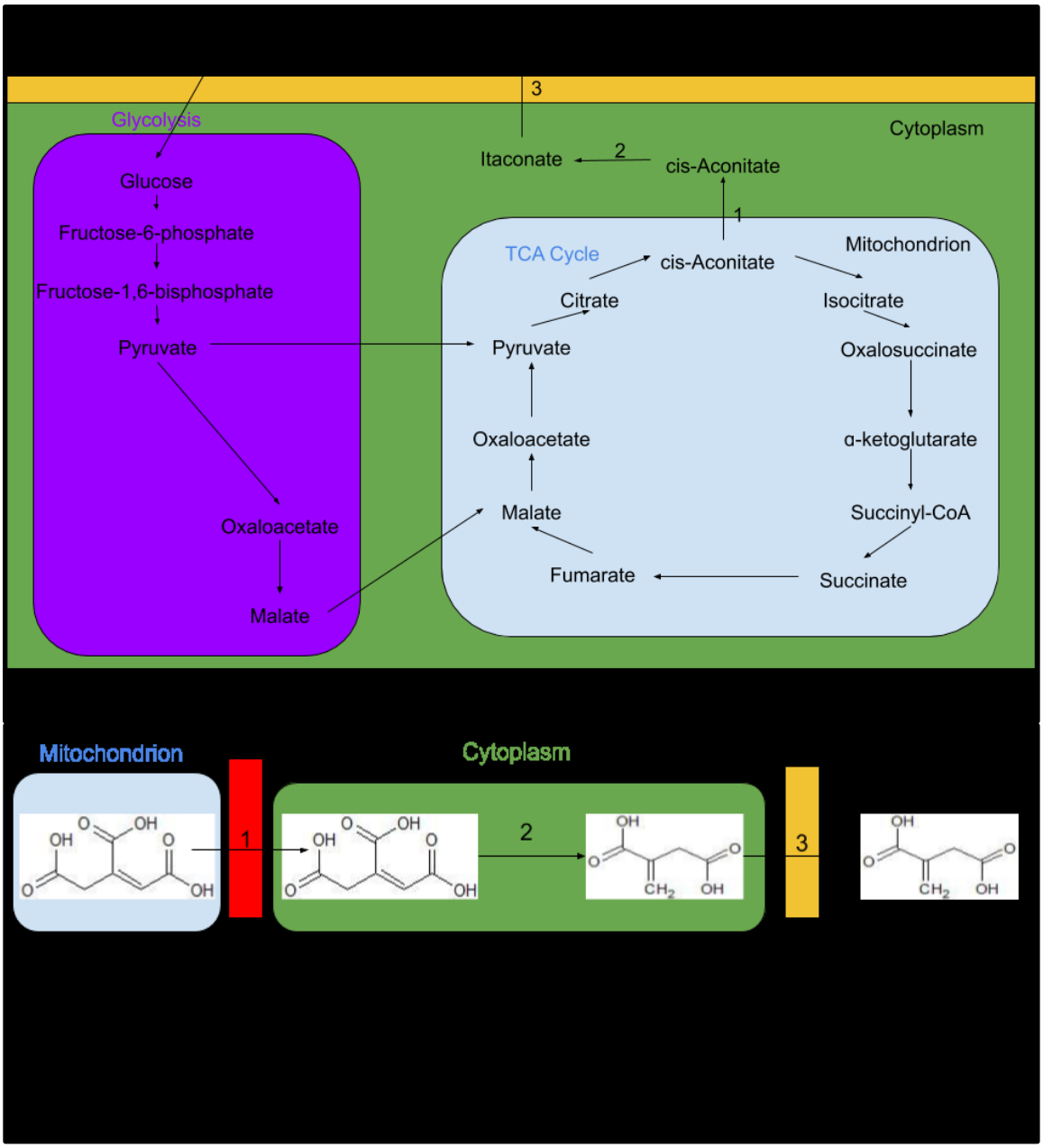

Optimization of Itaconic Acid Production in *A. terreus*

While gaps in the complete understanding of the biosynthetic process remain, there have nevertheless been extensive investigations carried out with the goal of

optimizing the production of itaconic acid in *A. terreus*. These investigations can be grouped into two main categories: process development, and strain improvement.

Process development began as soon as industrial production of itaconic acid started and continues to this day. This avenue of investigation focuses on the conditions of the fermentation itself and has resulted in optimization of the yield of itaconic acid by manipulation of factors such as high starting sugar concentration, pH control, extensive oxygenation of media, and manganese ion depletion [5,6,9,10,21,29].

Strain improvement investigations involve genetics, molecular biology and genomics-based techniques. These investigations center on the modification of *A. terreus* itself via the overexpression, knockout, or regulatory control of its genes, as well as random mutagenesis combined with specific screening [20,30–32]. One approach has been the overexpression of the itaconic acid cluster genes (*cadA, mfsA,* and *mttA*) as well as other genes that have been found to be upregulated during high levels of itaconic acid production [20]. Interestingly, the overexpression of the itaconic acid cluster genes produced only marginal increases in itaconic acid production, and while a set of genes with predicted effects on itaconic acid production were upregulated during periods of high itaconic acid production, all of these genes were expressed under low itaconic acid production conditions [20,28,33]. While gains have been made, the industrially relevant final titers of around 85 g/L are well below the theoretical maximum of 240 g/L[3,7,34,35].

Despite these investigations and a long history in the scientific literature *A. terreus* is still not nearly as well studied as other fully “modelized” organisms. This has led to some gaps in our understanding of *A. terreus* that make precise control of itaconic acid production rather difficult. However, there are other species of *Aspergilli* that have been investigated far more extensively where parallels may be relevant. One of these, *Aspergillus niger*, is an industrial producer of an organic acid; in this case citric acid which is a direct precursor of itaconic acid. Furthermore, *A. niger* has repeatedly been found to show parallels with *A. terreus* wherein modifications carried out in one of the

fungi have the same or similar effects in the other [10]. This is useful as *A. niger* has been investigated and genetically manipulated to a greater extent than *A. terreus* [3].

A. niger and Citric Acid Production

Commonly encountered as a mold that colonizes foodstuffs such as onions and peanuts, *Aspergillus niger* is named for the black spores it produces. It is a saprophytic soil fungus with global distribution. While it can adversely impact society both as a rare opportunistic pathogen and as a toxigenic contaminant of food products, several jurisdictions have denoted it as Generally Recognized As Safe (GRAS), or equivalent, provided that non-toxigenic strains are used. *Aspergillus niger*'s ecology as an organism that feeds on soil detritus relies on a wide variety of secreted enzymes to release nutrients from decaying plant matter. These same degradative enzymes have been repurposed for biotechnological processing of polymeric materials, such as starch, into simple sugars for use in food and other applications. While *A. niger*'s use for the production of proteins is of industrial interest, the first economically important application of *A. niger* was for citric acid production. [36,37]

Citric acid is a tricarboxylic acid of immense importance to human society. At room temperature it is a white crystalline powder with properties listed in Table 1. First discovered in 1784 by Carl Scheele as a constituent of lemon juice, it is present in a variety of citrus fruits [38]. While originally produced either from citrus fruit juice or chemical synthesis, microbial production using submerged fungus, primarily *A. niger*, is now the dominant means of satisfying the extensive worldwide demand. Globally, close to 2 million tons were consumed annually as of 2017, and the market value is expected to exceed 2 billion USD by 2020 [14]. Primarily used as an acidulant, natural pH regulator, and flavor in the beverage industry, it also has several other applications in the food, detergent, pharmaceutical, and other fields. The market value of citric acid and the projected growth of its global consumption have fueled continuing interest in the mechanism of its biological synthesis and the optimization of its production [39,40].

Like itaconic acid, citric acid is produced via the TCA cycle where it serves as an important intermediate of aerobic respiration in the primary metabolism of organisms [41]. Radiolabel tracer studies have demonstrated that it accumulates in *A. niger* as a product of the condensation of pyruvate with oxaloacetate [42]. Interestingly, later studies have demonstrated that glycolysis may not be the sole source of these precursors in *A. niger*, with noticeable quantities being produced from glycerol and erythritol [43] suggesting a strong likelihood that various side pathways may be operating under the carbon overflow conditions present during hyperproduction in *A. niger* [44]. Following its production in *A. niger* a series of transporters lead to the secretion of the accumulated citric acid into the extracellular medium[3]. While there is strong support for the identity of the enzymes responsible for the production of citric acid in *A. niger*[3,44] and good evidence for the primary citric acid transporters [40,45], the exact mechanisms of the regulation of citrate production in *A. niger* still merit further study [3].

Although the finer points of citric acid production in *A. niger* require further investigation, both *A. niger* and the microbial production of citric acid are better studied than *A. terreus* and itaconic acid production. Furthermore, higher titers and yields are observed for citrate production by *A. niger*, with titers approaching 360 g/L^{-1} [28] and yields up to 0.95 g per g glucose, very close to the theoretical maximum of 1.067 g citric acid per g glucose [46]. This is far superior to the current yields and titers of itaconic acid in *A. terreus* and suggest it may be possible to produce a final titer of 240 g/L itaconic acid as opposed to the currently achieved 85 g/L itaconic acid under industrially relevant conditions wherein glucose is continually added [28,35,47]. In *A. niger*, factors shown to affect production include: carbon source consumption, by-product control, inhibition of feedback loops, optimization of precursor pathways, respiration control, and the biochemical pathway itself, as reviewed by Tong et al.[46].

Genetic Manipulation of Filamentous Fungi

Genetic modifications in industrially useful filamentous fungi such as *A. niger* and *A. terreus* have a long history. Earliest efforts focused on isolating different strains with

properties that are most suitable for the process in question [48]. Following the Nobel Prize issued to Muller in 1946 for X-ray-induced mutagenesis, researchers had the tools necessary to create new strains of filamentous fungi through x-ray, UV, or chemical mutagenesis [49,50]. These methods could produce only random, unpredictable mutations until the dawn of molecular biology and the first protocols for the introduction of exogenous DNA and targeted deletions of endogenous DNA in the 1970s and 1980s [37]. In the 1980s effective and recyclable selection markers for filamentous fungi such as for arginine synthesis, hygromycin resistance, and uridine/uracil auxotrophy began to appear and come into use [51–53]. These systems, while effective, nonetheless required recycling of the selection marker and were limited in the number of loci available for targeting. Then in the early 2000s, genomes for filamentous fungi began to be available [54,55]. This allowed for far more extensive analysis and manipulation of not only individual species of filamentous fungi, but also comparative studies between species contributing to a rapid pace, depth and scope of research into these organisms [56,57].

CRISPR-Cas9

As genomic information has become available, so too have techniques for manipulating genomes. One of the most noteworthy recent developments has been the discovery and applied use of CRISPR-Cas9 genome editing [58,59].Originally discovered as an adaptive immune system in bacteria where it helps impart resistance to phage infections, it has been simplified and re-tooled as a means of introducing genetic modifications [60]. Cas9 is an endonuclease protein that causes double-stranded breaks in DNA, and CRISPR stands for Clustered Regularly-Interspaced Palindromic Repeats. These are DNA segment repeats that are generated from foreign DNA sequences and are used to create guide structures [60]. These guide structures consist of a scaffold which contains a short (20 bp) protospacer sequence that associates with a Cas9 protein causing it to recognize (through complementary binding of the guide RNA to target DNA) and cleave specific sequences of DNA [60]. Cas9 mediated DNA cleavage is both flexible and much more precise than previously developed methods [61]. It is flexible in that the system requires only a PAM (Protospacer-Adjacent Motif) consisting of NGG

directly downstream of the guide sequence. The guide sequence itself can be any 20-nucleotide section of the target's genomic DNA [62,63]. The Cas9-guide complex will then recognize this 20 bp sequence and cause a double-stranded DNA break, thus allowing for very predictable and specific DNA cleavage in the genome [59,63].

Such guided cleavages at specific genomic locations can then be used to induce modifications in the genome of the organism through its own endogenous repair pathways [64]. In eukaryotes there are two primary DNA repair systems; NHEJ (Non-Homologous End Joining) and HDR (Homology-Directed Repair) [59]. The NHEJ pathway involves direct ligation to repair breaks in genomic DNA. It is error-prone, often leading to small deletions or insertions in the sequence. These can cause alterations or losses of gene function through the introduction of frameshift and nonsense mutations [59]. Homology-Directed Repair on the other hand involves the use of a piece of DNA that is homologous to the broken strand as a template for repair of the break [59]. This pathway is much more accurate in its repair; hence precise changes or deletions can be accomplished by introducing a repair template with regions of homology around the cut site that either includes a new desired sequence for insertion or omits a region causing a deletion [59,63].

First reported in the *Aspergillus* genus in 2015 by Nodvig et al. [62] Cas9-based systems have now been adapted to at least five different species of *Aspergilli* using a range of different selection markers [59]. Its application has allowed for not only targeted deletions and insertions, but also specific regulatory control, and it has aided in the development of whole genome metabolic pathways [46,59]. However, despite its application in other *Aspergillus* species, to date, CRISPR-Cas9-based technologies have not yet been applied to *Aspergillus terreus*.

Specific Goals of This Investigation

As described above, many studies have been conducted on factors that affect citric acid production in *A. niger*. One such investigation sought to determine the genetic

differences between two strains of *A. niger*; a laboratory strain, NRRL 3 (ATCC 9029, CBS 120.49, NCIM 545, N400) and *A. niger* NRRL 2270 (ATCC 11414) which overproduces citric acid. *A. niger* NRRL 2270, a spontaneous mutant of the common industrial strain ATCC 1015 (NRRL 328, CBS 113.46, FGSC A1144, NCIM 588) [65]. A genetic comparison of the two strains revealed that the primary difference in terms of citric acid production may be three genes that were inactive in *A. niger* NRRL 2270, but active in *A. niger* NRRL 3 (A. Tsang, personal communication). It is hypothesized that knocking out orthologs of these genes in *A. terreus* could result in strains with improved production of itaconic acid. While ongoing research and intellectual property concerns have necessitated the omission of the specific identity of the genes this thesis still stands on its own as an exploration of the methods necessary to perform knockouts in *A. terreus*.

In order to construct such strains, CRISPR-Cas will be applied to *A. terreus* to create a strain with a suitable genetic marker to select for positive transformants, as well as carry out deletion of target genes. The use of CRISPR-Cas9 in *A. terreus* has not previously been reported, but since it has been applied successfully to other species of *Aspergillus*, it is anticipated that it should work once the right parameters have been determined. Construction of a suitable *A. terreus* selection strain will also be carried out using CRISPR-Cas9, and is based on systems that have been described previously [66].

Systems that have already been explored for construction of selection strains in *A. terreus* include acetamidase, albinism, and uridine/uracil auxotrophy [67,68]. However, none of these systems (indeed no experiments at all in *A. terreus*) have been published using CRISPR-Cas9 or extrachromosomal plasmid transformation. Re-constructing them using Cas9-based methods will provide proof of concept that CRISPR-Cas9 can work in *A. terreus* and is also a means of generating useful selection systems for subsequent experiments.

One very effective system used in *A. niger* is the aforementioned uridine and uracil auxotrophy [69]. Through the deletion of the gene encoding orotidine 5'-phosphate

decarboxylase (commonly referred to as *pyrG*), the ability to endogenously produce both uridine and uracil can be fully compromised, thus rendering the organism fully dependent upon supplementation of uridine and uracil in growth media for survival. A Δ*pyrG A. terreus* strain can be transformed with a plasmid vector containing *pyrG*, and transformants expressing the plasmid can be easily selected by simply plating them on media lacking uridine or uracil. However, as this is a loss of function mutation it requires the use of an additional selection marker in order to successfully introduce the second CRISPR-Cas9 plasmid that will lead to the deletion. The acetamidase (*amdS*) gene can functionally fulfill this role. Acetamidase allows filamentous fungi to effectively utilize acetamide as a sole nitrogen source whereas without this gene filamentous fungi grow very poorly using acetamide as a sole nitrogen source [70]. Furthermore, both *pyrG* and *amdS* can be counter-selected for the presence of the wild-type (*pyrG*) or integration of the transformation vector (*pyrG* or *amdS*). This is accomplished by supplementing media with either 5-fluoroorotic acid (for *pyrG* counter-selection) or fluoroacetamide (for *amdS* counter-selection): if an organism grown with these compounds harbors the active gene for their uptake and conversion it causes the endogenous production of highly toxic fluorinated metabolites [71,72]. To further evaluate the efficacy of the CRISPR-Cas9 plasmid system an additional gene will be targeted. The *melA (AtmelA)* gene in *A. terreus* encodes a NRPS-like enzyme responsible for producing the precursor to the organism's brown conidial pigment. Successful deletion mutants will therefore have white spores as opposed to the standard brown, allowing for easy visual scoring and distinction between transformants with a mutant versus wild-type phenotype [67]. While these genes have been used for selection of screening before in filamentous fungi, this would be the first time CRISPR-Cas9 has been used to generate corresponding mutations in *A. terreus* [6,67].

In summary, this investigation applied CRISPR-Cas9-based methods to *A. terreus* to first introduce a selectable marker into the wild-type strain for facile genetic manipulation, and then, tested the use of CRISPR-Cas9 to introduce deletions in the resulting strain, with the goal of eventually targeting an itaconate-overproducing phenotype.

Materials

Unless otherwise stated all reagents were procured from BioShop Canada (Burlington, Ontario), all restriction enzymes from New England Biolabs (Ipswich, Massachusetts), and all primers are from Integrated DNA Technologies (Coralville, Iowa).

Table 2: Media and Reagents

Complete Media (CM)	minimal media[73] supplemented with 55.5 mM glucose, 0.1% yeast extract, 0.1% casamino acids, and 10 mM L-uracil with a final uridine concentration of 1 mM (and a final agar concentration of 2% for solid media)
Aspergills terreus Cell Wall Digestion Solution	1.2 M $MgSO_4$ pH 5.6
DNA Extraction Buffer	17.3 mM sodium dodecyl sulfate (SDS), 10 mM Tris, and 128 mM ethylenediaminetetraacetic acid (EDTA) at pH 8.0
Malt Extract Agar (MEA)	2% Malt Extract, 4 mM Peptone, and 0.111 M D-Glucose (with a final agar concentration of 2% for solid media)
Non-Selective Regeneration Media (NSRM)	Minimal media[73] supplemented with 0.877 M sucrose, and 9 mM L-uracil with a final concentration of 1 mM uridine (and a final agar concentration of 2% for solid media)

Non-Selective Regeneration Media with Acetamide (NSRM + Acetamide)	Minimal media[73] with sodium nitrate omitted, supplemented with 0.877 M sucrose, and 9 mM L-uracil with a final concentration of 1 mM uridine and 4.5 mM Acetamide (and a final agar concentration of 2% for solid media)
Non-Selective Regeneration Media with Fluoroacetamide (NSRM + Fluoroacetamide)	Minimal media[73] with sodium nitrate omitted, supplemented with 0.877 M sucrose, and 9 mM L-uracil with a final concentration of 1 mM uridine and 4.5 mM fluoroacetamide (with a final agar concentration of 2% for solid media)
Non-Selective Regeneration Media with 5-fluoroorotic acid (NSRM + 5-FOA)	Minimal media[73] supplemented with 0.877 M sucrose, 9 mM L-uracil, and 7 mM 5-FOA with a final concentration of 1 mM uridine (with a final agar concentration of 2% for solid media)
Osmotic Stabilization (OM) Buffer	2.5 mM NaH_2PO_4, 13.1 mM Na_2HPO_4, and 0.768 M $MgSO_4$
PEG-TC	25% polyethylene glycol-6000 (Sigma Aldrich) in TC Buffer
Saline Tween	0.5% NaCl, 0.002% Tween 80
Selective Regeneration Media (SRM)	Minimal media[73] supplemented with 0.877 M sucrose (with a final agar concentration of 2% for solid media)
Sucrose Tris Calcium Chloride (STC) Solution	1.2 M sorbitol, 50 mM $CaCl_2$, and 10 mM Tris-HCl at pH 7.5

TB Layer	0.6 M sorbitol, and 0.1 M Tris-HCl at pH 7.5
Tris Calcium Chloride (TC) Buffer	50 mM $CaCl_2$, and 10 mM Tris-HCl at pH 7.5

Methods

Agarose Gel Electrophoresis[71]

Unless otherwise stated all gels are 0.8% agarose gels using the Invitrogen Generuler 1kb Plus DNA Ladder using standard methods[74].

Preparation of Spore Suspensions and Glycerol Stocks of *Aspergillus terreus* [75,76]

Glycerol stocks of *A. terreus* were prepared according to established procedures[75,76], as follows. Initial cultivation of *A. terreus* NRRL 1960 (Agricultural Research Service Culture Collection, Peoria IL) was carried out on Malt Extract Agar plates (pH 5) at 30°C or 37°C for ~7 days. Following this, plates were incubated at room temperature in darkness for ~48 hours to induce increased sporulation. Spores were suspended in saline-Tween and counted by eye using a hemocytometer to calculate concentrations of spores. Suspensions were mixed with glycerol to a final concentration of 50% and stored at -80°C for long-term use.

Genome Sequencing, Compilation, and Analysis

Genomic DNA of *A. terreus* NRRL 1960 was extracted by Sandrine Marqueteau and sequenced at the Genome Quebec Innovation Centre. A draft assembly of the full genome was constructed by Debra Fulton and compiled into an in-house BLAST[77] server by Alexandre Beaudoin.

Plasmid Construction [79]

Guides for CRISPR-Cas9 targeting of genes were identified using the “CRISPR Finding” program of the Geneious software (version R 9.1), and evaluated based on their Doench Activity Score, a method for predicting the efficacy of a particular guide sequence, low off-target risk, and position of the expected cut site within the coding

region (see Table 2). Inserts were constructed via fusion PCR and verified via observation of the correct band size [80].

Complete CRISPR guides were constructed from fusion PCR assembly of two fragments ("Fragment 1" and "Fragment 2") [79]. Specific guide primers were constructed corresponding to the 20bp guide sequence (PAM region was not included) with overlapping tail region for subsequent fusion PCR assembly. Fragment 1 included the upstream Ligation Independent Cloning sequence site, tRNA Promoter (Proline), and the specific CRISPR targeting sequence added to the 3' end via PCR. Fragment 2 included the added CRISPR targeting sequence at the 5' end and the tRNA terminator. Targets were amplified via PCR using a previously constructed CRISPR guide as the template. Correctly sized bands were excised, and column purified using the GE Healthcare Illustra GFX Gel Band Purification Kit, according to the manufacturer's instructions. Fragments were then inserted into an appropriate ANEp8-based plasmid for delivery into the cell, as described in the next section.

The previously-designed and constructed[66] ANEp8-*amds-cas9*-LIC plasmid (or ANEp8-*pyrG-cas9*-LIC, depending on which fungal selection marker is present) (see Figure 3 for plasmid map) was used in this investigation. Plasmids (500 ng) were digested with 25 U EcoRI restriction enzyme and visualized on agarose gels to verify and quantify plasmid. Purified ANEp8-*amds-cas9*-LIC plasmid (5ug/1 pmol) was digested for 4h at room temperature using 20 U of SwaI restriction enzyme, which cuts in the middle of the 38bp LIC site, in NEB Buffer 3.1 at a final volume of 100 µL, to linearize the plasmid. The linearized ANEp8-*amds-cas9*-LIC plasmid and the assembled insert were then treated with T4 DNA polymerase to generate complementary single stranded overhangs. For the plasmid mixture, 0.133 pmol of linearized plasmid was treated with 3 U of T4 DNA polymerase, 0.8 µL 0.1M dithiothreitol, and 2 µL 25 mM dGTP (to arrest exonuclease activity at a specific site), in NEB Buffer 2.1 in a final volume of 20 µL. For the insert mixture, 4.5 pmol of assembled insert was treated with 3 U of T4 DNA polymerase, 0.8 µL 0.1M dithiothreitol, and 2 µL 25 mM dCTP (to arrest exonuclease activity) in NEB Buffer 2.1 at a final volume of 20 µL. Both reactions were

carried out at 22°C for 35 min followed by 20 min at 72°C to deactivate the T4 enzyme. To anneal the two pieces, 4 µL of the T4 treated insert (~1.55 pmol ends) was combined with 2 µL of T4 treated vector (~0.025 pmol ends) and annealed using a thermocycler set to 60°C with a negative ramp of 0.1°C per second down to 4°C.

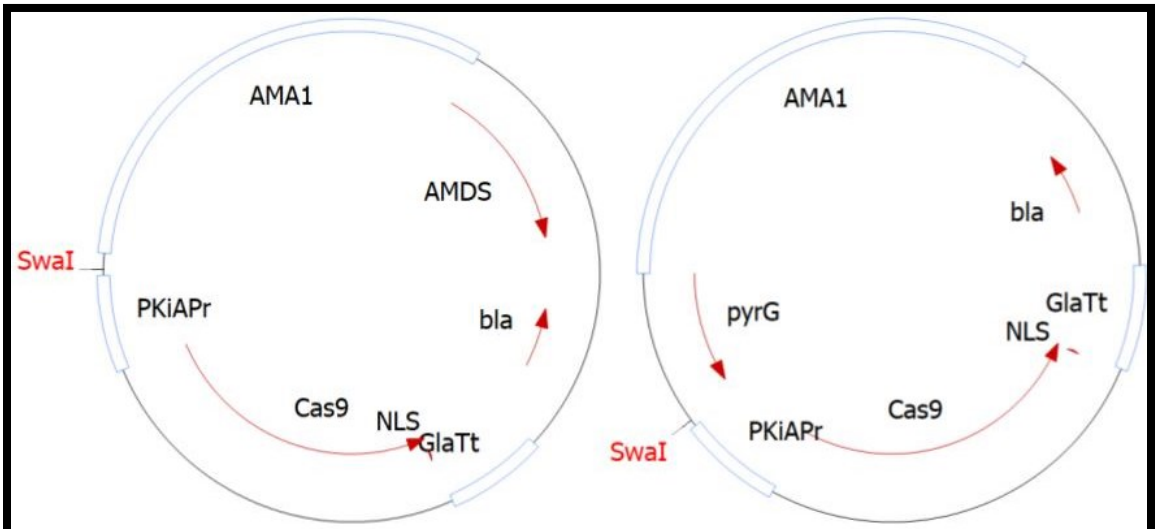

Figure 3: Plasmid Maps of Ligation-Independent Cloning Compatible Cas9 Plasmids. The Cas9 plasmids used in this investigation with fungal selection markers acetamidase (*A. nidulans* AmdS, Left), and orotidine 5'-phosphate decarboxylase (*A. nidulans pyrG*, Right). The red SwaI restriction enzyme cut site is the LIC site. Abbreviations are: AMA1 (plasmid replicator sequence of *A. nidulans*), bla (beta-lactamase ampicillin resistance gene for bacterial selection), GlaTt (*A. niger* Glucoamylase gene terminator sequence), NLS (nuclear localization signal), and PKiAPr (*A. niger* Pyruvate Kinase gene promoter sequence)[61] . Diagram constructed using Clone Manager 9

Assembled plasmids were transformed into competent *E. coli* DH5α cells, as described [81]. Two distinct colonies were picked from each plate and screened for the presence of transformed plasmid with insert via colony PCR. Colonies were picked and DNA was extracted using the Bio Basic Plasmid Miniprep extraction kit as per manufacturer's instructions.

Extracted plasmids were analyzed via PCR and restriction enzyme digestion. For PCR analysis primers used were either common to the plasmid flanking the LIC site or specific to the insert (see Figure 4). For the Cas9 plasmid with no insert to target Cas9 to a specific region in the genome, primers (black arrows) are specific to a region of the

plasmid flanking the LIC site (red line) where the insert is introduced: PCR reaction gives a 131 bp fragment corresponding to an empty vector (Figure 4A). For the Cas9 plasmid (ring) with a guide insert (purple wedge) introduced at and replacing the LIC site, the same primers as in A (black arrows) amplify a region flanking the insert: introduction of the insert results in a larger PCR product of 490 bp (Figure 4B). For the Cas9 plasmid (ring) with a guide insert (purple wedge) introduced at and replacing the LIC site, one common forward primer (black arrow) and a reverse primer (purple arrow) specific to an individual guide insert ensures only a plasmid with that specific guide inserted will give a product: expected size of the PCR fragment is 280 bp (Figure 4C). For specific primers used see Table S1.

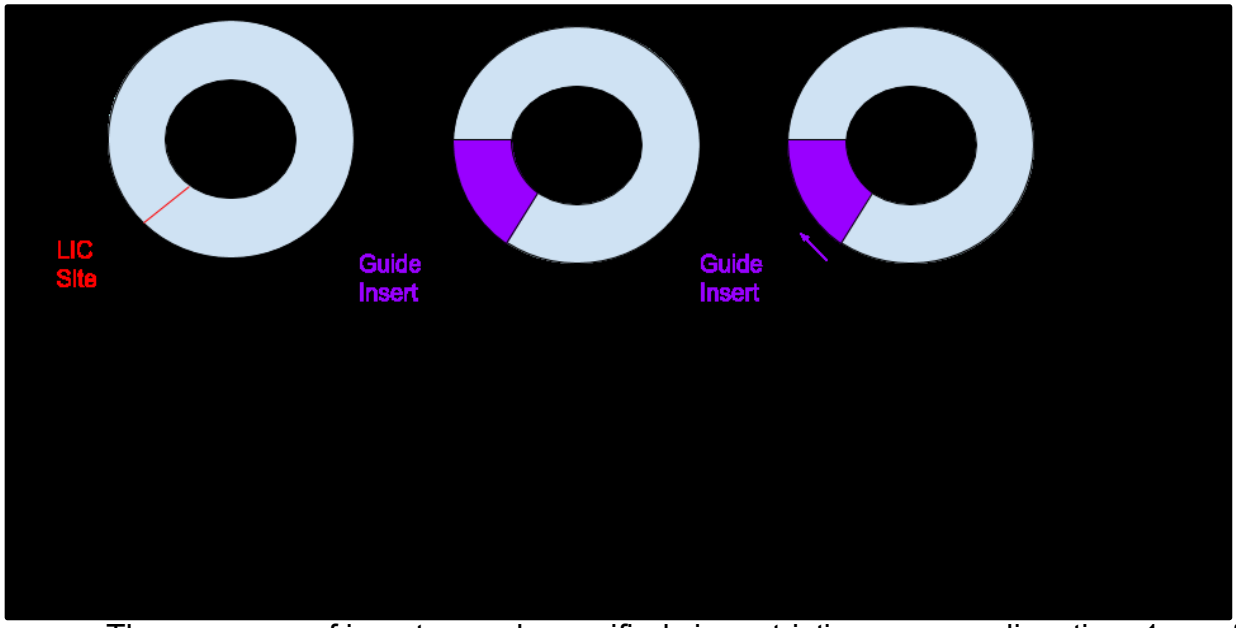

The presence of insert was also verified via restriction enzyme digestion: 1 µg of plasmid was incubated with 10 U of SmaI restriction enzyme at 25°C for 30 min. There are two SmaI restriction sites in an empty vector, and three SmaI restriction sites in a vector that has had a guide insert introduced. Identity of plasmid was further verified via digestion of 1 µg of plasmid with 10 U of EcoRI restriction enzyme at 37°C for 30 min. Confirmation of the appropriate digestion fragment sizes was carried out by imaging following agarose gel electrophoresis. For expected band sizes see Figure 8.

It has been reported that homology-directed repair templates (HDRTS)

with large (~1kb) homology flanks corresponding to the regions upstream and downstream of a target area, but omitting the target area itself, can be used to cause large, predictable deletions with high efficiency [63]. Primers were designed for the amplification of ~900bp portions upstream and ~900bp portions downstream of the *A. terreus* genome harboring the gene to be deleted (Figure 5A). The reverse primer of the upstream region and the forward primer of the downstream region included an LIC region (purple tails on primers, Figure 5A). Following amplification of the upstream and downstream fragments from *A. terreus* genomic DNA, the fragments were annealed and amplified to create the final ~1.8kb repair templates (see Figure 5 B-D) which have homology to the regions upstream and downstream of the gene of interest but omit the gene itself: the result is total deletion of the gene should it be incorporated following the transformation (see Figure 6). Products were visualized following agarose gel electrophoresis, and bands of the desired size were gel purified to remove template and incomplete products.

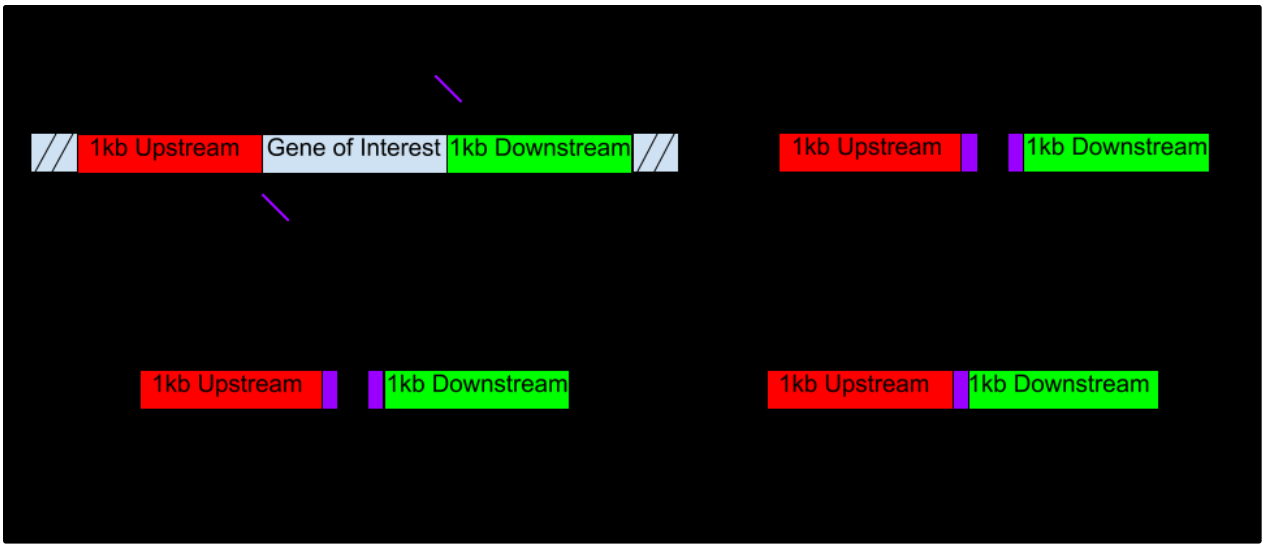

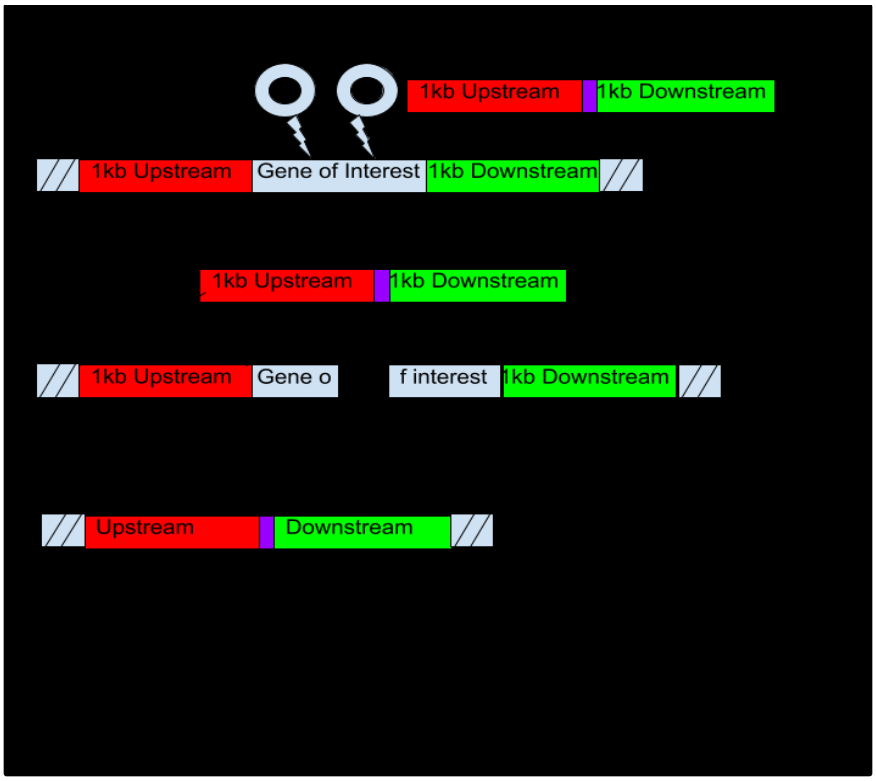

A. terreus Protoplast Preparation and Δ*pyrG* Transformation [82]

A suspension of *A. terreus* spores was used to inoculate 50 mL of Complete Media (CM) to a concentration of $1*10^6$ spores per mL, and grown for 16h at 300 rpm and 30°C. Mycelia were collected via Miracloth filter and washed one time with digestion buffer. Vinotaste Pro (Novozymes) lysing enzymes were dissolved in digestion buffer to 100 mg/mL and sterilized via filtration (0.45 µM pore size). Two grams of washed mycelia were suspended in 10 mL of filter-sterilized digestion buffer and lysing enzymes, and incubated at 150 rpm and 37°C for 16h. Following digestion, the presence of protoplasts was visually evaluated via light microscope at 40X magnification. Protoplasts were collected by pouring the mixture through a Miracloth filter into a 50 mL conical tube and 10 mL STC was added. Samples were centrifuged for 10 min at 2000 x g and 10°C. Supernatants were decanted and the pellets were resuspended in 1 mL STC. Sample was transferred to a microfuge tube and centrifuged for 5 min at 2300 x g to wash protoplasts. The wash step was repeated twice. After the final wash step, protoplasts were resuspended in ~500 µL STC and counted. Thirty to

one hundred protoplasts were plated on NSRM to evaluate survival rate. For transformation, 100 µL of protoplasts was transferred into a 5 mL tube for each sample. Plasmid DNA (Anep8-*amdS-cas9* [gRNA targeting *pyrG*]) was added to each sample (20 µL dd H_20 for negative control, 500 ng of empty plasmid vector for positive controls, and 500 ng of plasmid with deletion insert for experimental trials), and incubated on ice for 15 min. PEG-TC (500 µL) was added to each sample and incubated for exactly 5 min, then rescued with 1 mL of STC. Transformation mix was plated on SRM selective media (up to 1 mL per plate) and incubated at 30°C until colonies were observed.

Prospective Δ*pyrG* transformants were isolated from NSRM + Acetamide transformation plates by size differentiation from background colonies to select for the presence of the acetamidase gene. This gene is used as a selection marker which results in better utilization of nitrogen from acetamide, and therefore distinct colonies. Spores were picked from colonies using a wet toothpick, diluted down to ~100 spores, and replated on NSRM-Acetamide. Positive colonies were identified based on size differentiation and the process was repeated until no background was discernible. Isolated positive colonies were then plated on NSRM + 5-FOA to select for a phenotype with a defective *pyrG*. Colonies with good growth were tested for auxotrophy by replating on media with and without uridine. Once transformants were isolated which displayed good growth with uridine and no growth without uridine, one transformant sample was selected for gDNA extraction. The colony was picked and used to inoculate 10 mL of Complete Media. The culture was grown overnight at 37°C with 220 rpm shaking. The following day, mycelia were collected and washed once with ddH_2O. Mycelia were suspended in 800 µL DNA Extraction Buffer and disrupted using a MP FastPrep 24 using 425-600 µM glass beads with a velocity of 6 m/s for 60 sec per run and four runs conducted. DNA was then extracted using the phenol-chloroform method[83]. The region of the genome corresponding to *pyrG* was PCR-amplified and sequenced to determine the specific nature of deletion mutation present (for specific primers used see Table S1).

Following isolation and genotype confirmation of the *A. terreus* strain with a disrupted *pyrG* gene, it was investigated for the full removal of the extrachromosomal transformation plasmid, and the phenotype. The strain was plated on various selective media to confirm auxotrophy and the absence of the acetamidase selection marker. Comparison plates with 200 wild-type and 200 Δ*pyrG* spores normalized to 2 µL volume were spotted on SRM, NSRM, NSRM + acetamide, NSRM + fluoro-acetamide, and NSRM + 5 FOA. The selection pressures presented by these media are as below (Table 3).

Table 3: Verification of Removal of Δ*pyrG* Plasmid from Δ*pyrG* Selection Strain [72]

Media	Media Composition	Selection Pressure
SRM	minimal media (with high sucrose concentration) with no uridine or uracil	Organisms lacking a functional *pyrG* would not grow
NSRM	Minimal media (with high sucrose concentration) supplemented with uridine and uracil	No selection pressure
NSRM + Acetamide	Minimal media (with high sucrose concentration) supplemented with uridine and uracil, nitrogen source has been replaced with acetamide	If the organism contains the acetamidase gene it should grow well, otherwise it should display a “starvation” phenotype

NSRM + fluoro-acetamide	Minimal media (with high sucrose concentration) supplemented with uridine and uracil, nitrogen source has been replaced with fluoro-acetamide	If the organism contains the acetamidase gene it should die (as a result of the generation of toxic metabolites from fluoro-acetamide), otherwise it should display a "starvation" phenotype
NSRM + 5-FOA	Minimal media (with high sucrose concentration) supplemented with uridine and uracil, additionally supplemented with 5-fluoroorotic acid	An organism that lacks a functional *pyrG* should grow, the wild-type should show no growth

Plates were incubated at 37°C and observed for growth trends.

Aspergillus terreus Protoplast Preparation and Target Genes Transformation Using HDRTs [63,82]

Knockouts of targeted *A. terreus* genes were performed as above with the following modifications. Spore concentration was increased to $2*10^6$ spores per mL. In addition to VinoTaste Pro enzymes (Novozymes) (70 mg/mL), *Trichoderma harzianum* lysing enzymes (Sigma Aldrich) were also used (20 mg/mL) during protoplast preparation. Additionally, digestion time was shortened to 4h, and centrifugation was performed at 4°C for 30 min with floating protoplasts isolated as opposed to pellet. Two Cas9 plasmids with inserts targeting a specific gene of interest were co-transformed with a Homology-Directed Repair Template (HDRT) constructed for that specific gene (see Figure 6). Following the Cas9-induced double stranded DNA break and subsequent repair utilizing the HDRT, the gene of interest should be cleanly removed with the only other alteration to the genome being the addition of the short synthetic sequence used to assemble the HDRT. The amount of plasmid DNA transformed was increased to 1.1-1.8 µg total (equal amounts of each of the two plasmids targeting that gene) for targeted

knockouts and 1.5 µg total was used for the Vector Transformant Only (VTO) control, which was transformed with only the parent ANEp8-*cas9-pyrG*-LIC plasmid with no insert for Cas9 targeting or co-transformed repair template. Each gene of interest transformation also received 10 µg of repair template DNA. Growth was carried out on SRM (media lacking uridine or uracil) at 37°C.

Screening of Targeted Gene Knockouts

Ten colonies from each transformation plate (30 colonies total plus controls) were selected for initial screening. Colonies were picked for each prospective mutant and used to inoculate 10 mL of Complete Media. Cultures were grown overnight at 37°C with shaking at 220 rpm. The following day mycelia were collected and washed once with ddH_2O. Mycelia were suspended in 800 µL DNA Extraction Buffer and disrupted using a MP FastPrep 24 with 425-600 µM glass beads at a velocity of 6 m/s for 60 sec per run with 4 runs conducted. Genomic DNA was extracted twice using Phenol/Chloroform equilibrated to pH 7.9. DNA was recovered via Isopropanol precipitation and resuspended in Nanopure water. Genotyping was performed via PCR amplification of the gene of interest using primers spanning the expected deletion site, as described above. Following generation of results for the initial 30 colonies an additional 8 colonies from one of the genes of interest deletion transformations were screened as above.

Knockout of the *A. terreus melA* gene (responsible for conidial pigment production) was performed as described for the knockout of the targeted *A. terreus* genes, with slight modifications. Two Cas9 plasmids with inserts targeting the *melA* gene (see Figure 3 and Table 2) were co-transformed. The amount of plasmid DNA transformed was 1 µg total (500 ng ANEp8-*cas9*[*ΔmelA*$_1$]-*pyrG* + 500 ng ANEp8-*cas9*[*ΔmelA*$_2$]-*pyrG*) for the *melA* knockout, and 1 µg was used for the Vector Transformant Only (VTO) control, which was transformed with only the parent ANEp8-*cas9-pyrG*-LIC plasmid with no insert for Cas9 targeting. Only plasmid DNA was

transformed with no repair template. Additionally, a no DNA negative control was carried out.

Screening and isolation of prospective Δ*melA* strains was carried out by visual observation. Colonies showing production of white spores were picked, spores were suspended in saline-Tween, and ~30 spores were plated on NSRM and grown at 37°C. Two successive rounds were carried out until only colonies showing white spores were observed.

Following the initial transformation, the experiment was re-performed as above with a separate batch of protoplasts and plasmid DNA (ANEp8-*cas9*[Δ*melA*$_2$]-*pyrG*) at concentrations of 500, 1000, 1800, 2000, 2500, and 5000 ng per conditions.

Results

Aspergillus terreus Gene Target Identification

Due to the preliminary nature of the *A. terreus* NRRL1960 genome scaffold assembly, direct generation of gene targets using comparison with the sequences of corresponding *A. niger* genes was not usually possible. Therefore, gene targets were selected by first using BLASTP (Compositional Matrix adjust method), with the *Aspergillus niger* protein sequence as the query, against the publicly-available genome sequence of the NIH 2624 strain of *A. terreus*[78] via NCBI BLAST. Analysis of the 3 *A. niger* NRRL3 genes of interest gave one result each of *A. terreus* NIH 2624 sequences (designated “orthologs A, B and C”) with compelling similarity to *A. niger* orthologs. The highest scoring homologs in the *A. terreus* NIH2624 strain were then used to identify matches in the *A. terreus* NRRL 1960 scaffold. The actual *A. terreus* NRRL1960 targets were determined using a nucleotide-nucleotide alignment (BLASTn) with the NIH2624 strain as the query. These regions were used as the prospective genes targeted for deletion experiments. As the identity of the *A. niger* genes has not yet been publicly disclosed the identities and sequences of the *A. terreus* orthologs has been omitted from this thesis. The actual sequences used are immaterial for the purposes of interpreting the experiments presented here, which were directed at demonstrating whether or not the CRISPR-based methodology developed to knock out *pyrG* also works to further delete targets in the *A. terreus* genome.

CRISPR-Cas9 Guide Identification

Two types of genes were targeted: those associated with the construction of the selection/screening strains, and those implicated in organic acid production. Contig homologs were used to develop guides with the full *A. terreus* NRRL 1960 scaffold assembly as the genome guide. Targets with off-target effects corresponding to low numbers of mismatches were disregarded to help correct for possible errors attributable to the preliminary nature of the NRRL 1960 assembly. All guides were manually checked against the genome sequence of the publicly-available *A. terreus* NIH 2624 strain[78] to ensure the guides were targeted within the coding region of the genes of

interest. Overall, 9 guides were selected (1 targeting *pyrG* and 2 for each of the 3 prospective itaconate-related genes, and 2 targeting *melA* see Table 3). Each guide included 23 base pairs: 20bp of guide sequence (later used as gRNA) plus 3bp Protospacer Adjacent Motif sequence (which was not included in final gRNA construction).

Table 4: Genes Targeted and Guides Used (*Aspergillus niger* Orthologs Omitted)

Gene Name	*Aspergillus terreus* NIH 2624 Analog	Gene Location (*A. terreus* NRRL1960 Scaffold Assembly)	Guide Sequence (PAM Included)	Guide Location (relative to start of gene)	Guide Activity (Doench 2014)
pyrG	ATET_09675	Contig31:71633-70752	GCGCGCTGCGCATCTCCGAGTGG	380-402	0.48
melA	ATET_03563	Contig12:3299-6076	GCGAGAGCGTATGGTCCGTGCGG	2189-2167	0.779
			TGGATTGTTTGAAAACGCAGGGG	294-272	0.681

Aspergillus terreus Protoplast Preparation Optimization

Several protocols for the preparation of *A. terreus* protoplasts suitable for transformation with plasmid DNA are available in the literature [6]. As none of the published protocols attempted were immediately successful in generating transformable protoplasts, an optimization of the in-house *A. niger* transformation protocol[82] was carried out to generate a working transformation protocol for *A. terreus* NRRL 1960. Developmental stage of *A. terreus* culture, digestive enzyme mix, buffer used, and method of protoplast purification were all varied to generate the final protocol described in “Materials and Methods”.

In the course of developing the transformation protocols, pilot experiments were performed using different digestion buffer solutions to evaluate the efficacy of a shortened protocol using increased enzyme concentrations. It was determined that SMC was completely ineffective (0 transformants/µg), OM was less effective than the initial method (2.67 transformants/ µg), and that 1.6 M $MgSO_4$ offered a slight improvement initially (14 transformants/ µg). Following an increase of the spore concentration to $2*10^6$ spores per mL from $1*10^6$ spores per mL and the use of *Trichoderma harzianum* lysing enzymes (suggestion of Dr. Jean-Paul Ouedraogo) this transformation protocol yielded an efficiency of 66.9 transformants/ µg (standard deviation of 7.71). Over all experiments performed in relation to this thesis resulted in an improved protocol that had an average efficiency of 114.5 transformants/ µg (standard deviation of 57.03), whereas the initial transformation protocol used to generate the *pyrG* deletion strain had an average efficiency of 9.90 transformants/ µg (standard deviation 13.12).

Aspergillus terreus Selection Strain Construction

Prior to generating targeted genome knockouts, a host strain of *Aspergillus terreus* NRRL1960 suitable to receive CRISPR-Cas9 plasmid constructs was created. Given its successful application in *A. niger*, the approach taken is based on introducing auxotrophy of uridine and uracil through the deletion of the *A. terreus* gene (*pyrG*) encoding orotidine-5'-phosphate decarboxylase. The resulting Δ*pyrG* strain cannot grow on medium that does not contain uridine and/or uracil. The Δ*pyrG* strain may then be used to receive plasmids containing *pyrG* as a selection marker and selected for by plating on media lacking uridine/uracil and picking colonies that grow.

PyrG Target and Guide Construction: The gene (*pyrG*) encoding orotidine-5'-phosphate decarboxylase in *Aspergillus terreus* NIH2624 was used to identify a region of Contig 31 as the prospective *pyrG* gene in *A. terreus* NRRL1960 (see Methods). Designed guides (Table 3) were successfully assembled via fusion PCR, and the 375 bp appropriate size was verified using PCR and agarose gel electrophoresis (see Methods). An insert targeting *pyrG* was then introduced into the ANEp8-*amdS-cas9*-LIC2 plasmid which

uses the acetamidase (*amdS*) gene as a positive selection marker by improving a recipient organism's ability to utilize acetamide as a sole nitrogen source. The resulting plasmid was transformed into *E. coli*.

Plasmid Construct Verification: Following transformation, *E. coli* colonies demonstrating ampicillin resistance were screened for the presence of the correctly-assembled plasmid through colony PCR and restriction enzyme digestion. Colony-PCR using primers specific to the plasmid external to and flanking the insert site verified the presence of an insert, as described in *Methods*. The forward primer binds at bp 10047-10065 on the parent plasmid, and the reverse primer binds at bp 10155-10177 on the parent plasmid, spanning the LIC site at bp 10110. With no insert present (such as in the case of the parent plasmid) a product 131 bp in size is generated, however if the 359 bp insert has been correctly introduced the product size is then 490 bp. Following colony PCR only those colonies which produced a 490 bp product (Figure 7) were used for additional screening.

The identity of the guide introduced was verified using a common forward screening primer which binds at bp 10047-10065 and a reverse primer specific only to the designed and generated Δ*pyrG* guide at bp 10326-10345 (after integration of insert, see Figure 4). A plasmid with the correct guide inserted will produce a 280 bp result. Both PCR screens resulted in correctly sized bands as imaged on agarose gels (Figure 7). The size and identity of the plasmid was further confirmed via restriction enzyme digestion by two different enzymes, EcoRI and SmaI (see *Methods*). EcoRI produces bands of 7554, 6954, and 2277 bp. SmaI produces bands of 14207, 1554, and 1015 bp: additionally one of the restriction sites for SmaI is only present in the insert region serving as an additional indicator of insert integration. Both enzyme digests produced all expected bands at the appropriate size (Figure 8A-B). The resulting plasmid, now designated ANEp8-*amds-cas9*(Δ*pyrG*), was used in the deletion of the *pyrG* gene of *A. terreus* NRRL1960. For a full description of the full design and sequence of the parent plasmid see the original publication [66].

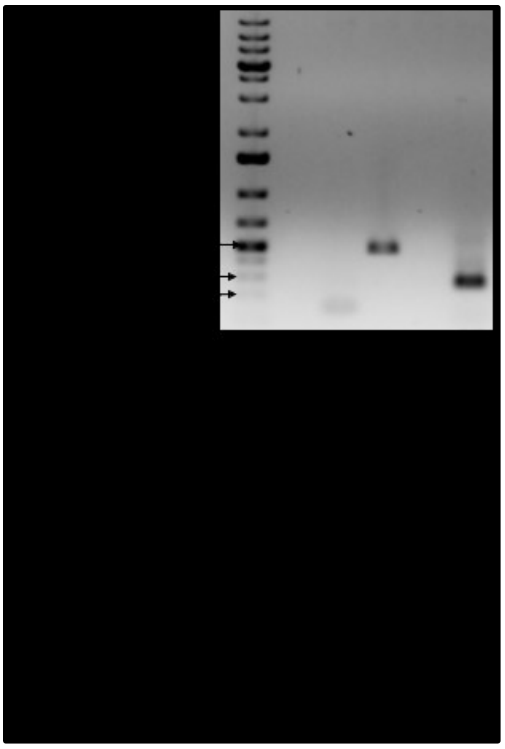

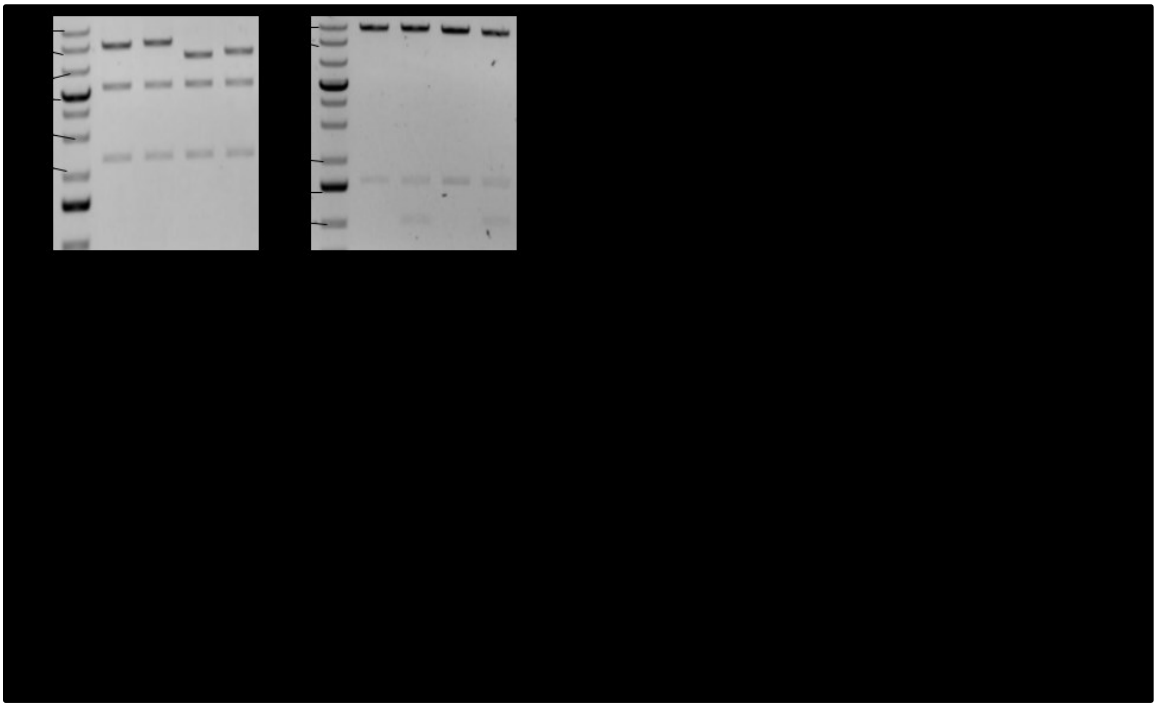

Construction of *A. terreus* Δ*pyrG* Selection Strain: Transformation of wild-type *A. terreus* NRRL1960 with the ANEp8-*amdS*-*cas9*(Δ*pyrG*) plasmid yielded 39 total transformants

as determined by the presence of large mature colonies grown on plates with acetamide as the sole nitrogen source (Figure 9). This indicates expression of the acetamidase gene of the introduced plasmid, and therefore, successful incorporation of the plasmid to *A. terreus*. A “haze” of stunted colonies was also observed but disregarded as background and not considered true transformants (see Figure 9).

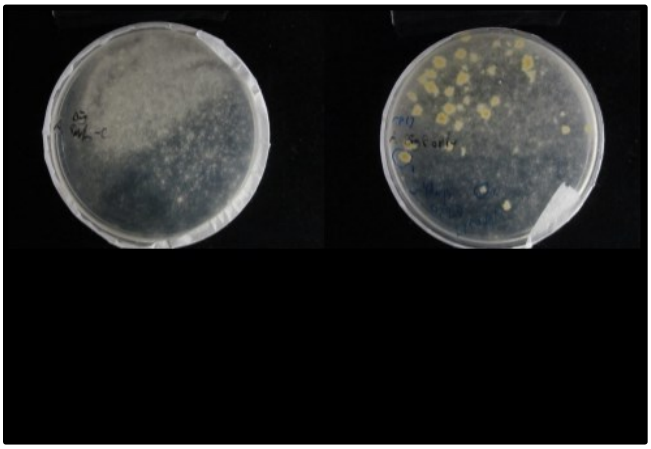

Selection and purification of *A. terreus* Δ*pyrG* Strains: Transformants were further screened based on their ability to grow on media containing 5-FOA. 5-FOA is incorporated by organisms with a functional *pyrG* gene and converted into highly toxic metabolites that kill the cell. However, organisms with a defective *pyrG* gene are resistant to 5-FOA. Purified *A. terreus* colonies transformed using plasmids with a functional Cas9 insert in the previous step were replated on NSRM + 5-FOA, and colonies that sporulated after approximately 3 weeks of growth at 30°C were selected. After this initial round of 5-FOA selection all transformants showed reduced growth when plated on standard minimal media lacking uridine and uracil as compared to the wild-type but not complete auxotrophy (data not shown). Control transformants produced using plasmids with no functional Cas9 insert did not demonstrate any auxotrophy or germination on plates containing 5-FOA (data not shown). After a second round of 5-FOA selection, all transformants showed an inability to grow on media lacking uridine (Figure 10). This complete and stable auxotrophy indicates a fully inactivated *pyrG* gene in these transformants.

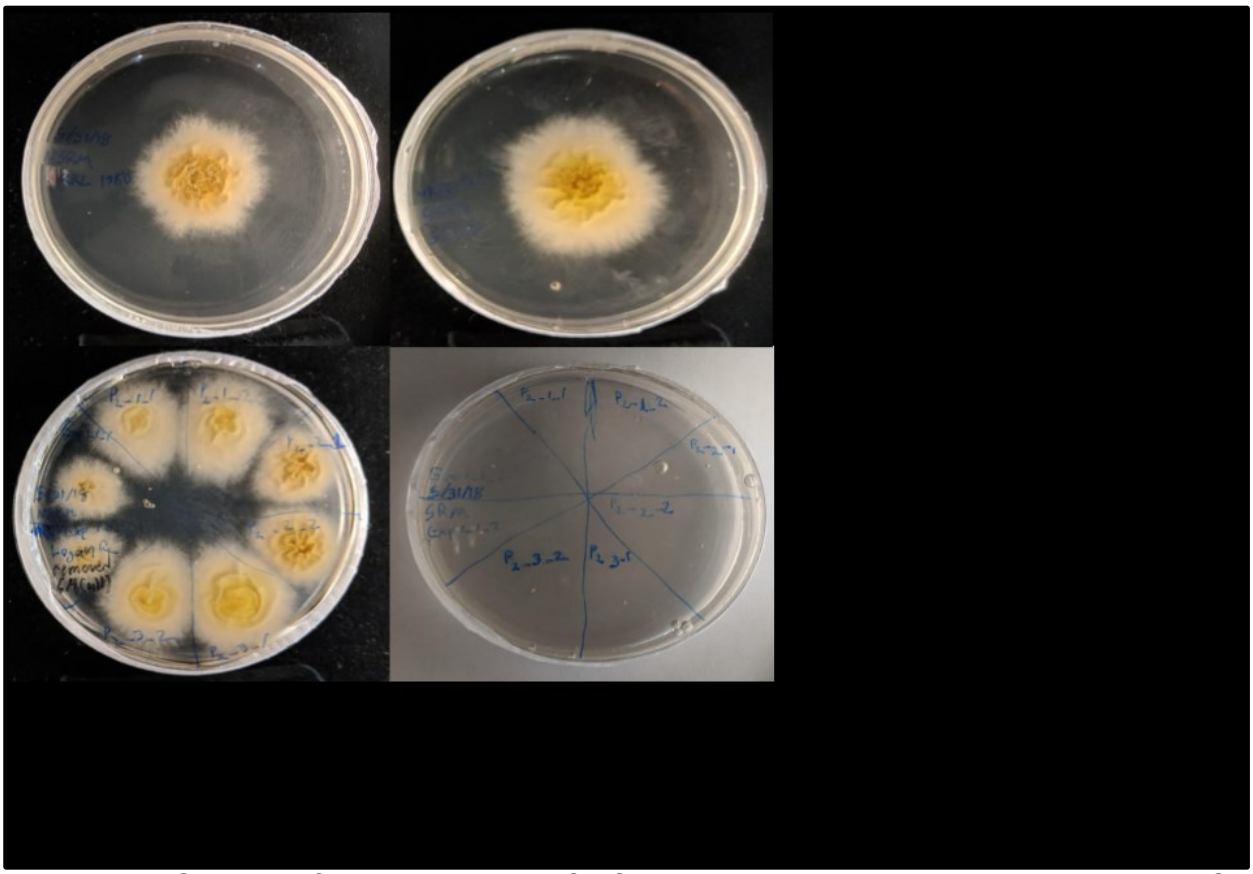

One transformant, selected for further development, was checked to see if the *pyrG* deficiency could be reversed by the re-introduction of the *pyrG* gene. Transformation of this strain with a *pyrG*-containing plasmid (ANEp8-*cas9*-*pyrG*-LIC) regenerated prototrophy as displayed by the transformant's ability to grow in media lacking uridine and uracil, whereas a negative control which received no plasmid remained completely auxotrophic with respect to uridine and uracil (Figure 11). This indicates the observed auxotrophy is a direct result of the inactivation of the *pyrG* gene.

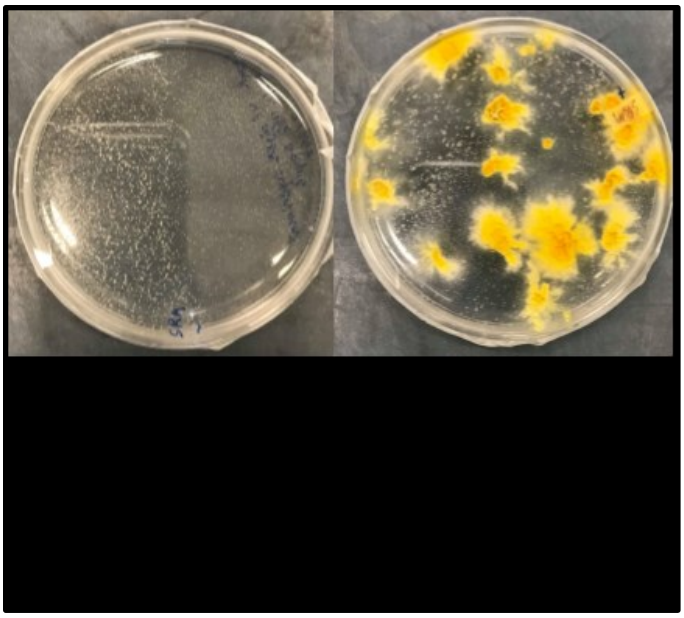

Sanger sequencing of the *pyrG* gene of the prospective mutant gave sequences for an 862 bp fragment (Forward) and an 846 bp fragment (Reverse). The two sequences showed identical high confidence results over the region targeted by the Cas9 guide. Alignment of the obtained sequences showed perfect agreement between themselves and generated an 800 bp consensus region. This region showed perfect identity to the wild-type *A. terreus pyrG* (Contig 31) gene, with the exception of a 76 bp insertion, 75 bp of which is a portion of the *blaA* gene, inserted at site 4-5 (Figures 12 (orange letters) and 13). This insertion is consistent with a Cas9-induced double-stranded DNA break (Figure 12) [66]. Since this 75 bp region shows perfect identity to a portion of the *E. coli blaA* region present in the ANEp8-*cas9*-LIC2 plasmids (Figure 14), it appears that part of the vector sequence was integrated at the double-stranded break. The additional C-base could be a result of an error introduced during repair of the chromosome break. This mutant maintained auxotrophy throughout the course of all observations, and over several generations. As a result, this mutant was maintained and used as the Δ*pyrG* selection strain in later experiments.

Additionally, two other prospective mutants (Figure 10) were sequenced. The sequences of these two mutants indicate single bp insertions 5 and 4-7 bp upstream of the PAM site (FIgures 15 and 16).

TTGCAGGACCACTTCTGCCTCGGCCCTTCCGGCTGGCTGGTTTATTGCTGATAAATCTGGAGCCGGTGAGCGTGC

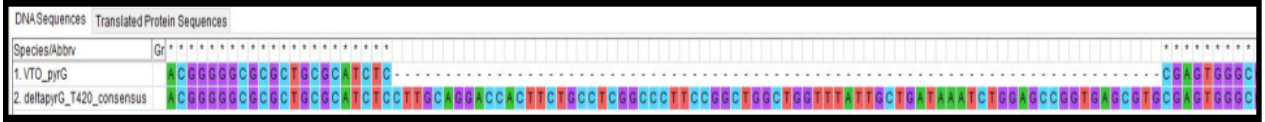

Orange

red

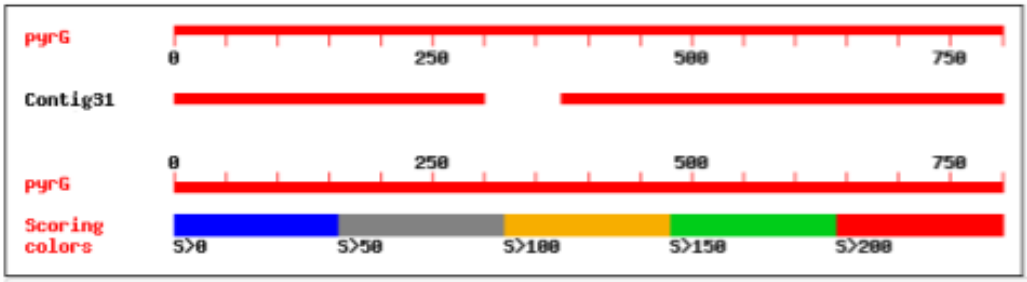

> Contig31

Length=342341

Score = 553 bits (299), Expect = 8e-157
Identities = 299/299 (100%), Gaps = 0/299 (0%)
Strand=Plus/Minus

Score = 787 bits (426), Expect = 0.0
Identities = 426/426 (100%), Gaps = 0/426 (0%)
Strand=Plus/Minus

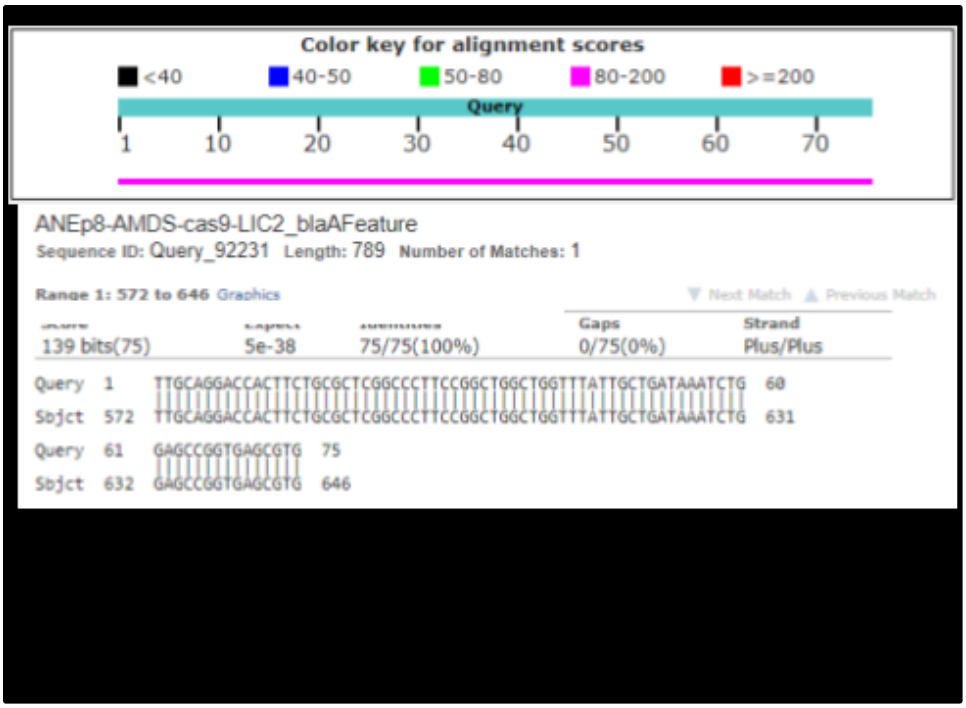

>deltapyrG_P2_1_1_consensus

CGAACGTGACGGTGTCGGCGGACGTGTCGACGACGAAAGAGCTGCTGGACCTTGCCGACCGTAGGACTCT
CGCCGCAGCCATAGACTCGGAATACTAAACGCAGACGACAGGCCTCGGACCGCACATTGCCGTGATCAAGA
CGCACATCGACATCCTCTCGGACTTTAGCGACGAGACGATCCGCGGGCTGAAGACGCTCGCGGAGAAGCAC
AACTTCCTCATCTTCGAAGACCGCAAGTTCATCGACATCGGCAACACGGTGCAGAAGCAGTACCACGGGGG
CGCGCTGCGCATCTCAC*GAG**TGG**GCGCACATTATCAACTGTAGCGTGCTGCCCGGCGAGGGCATCGTCGA
GGCACTCGCCCAGACCGCCGCGGCGCAGGACTTCCCCTACGGCCCGGAACGTGGCCTGCTCATCCTCGCC
GAGATGACCTCCAAGGGGTCGTTGCCCTACGGCCCGGAACGTGGCCTGCTCATCCTCGCCGAGATGACCTC
CAAGGGGTCGTTGGCGACGGGCCAGTACACAACTGC

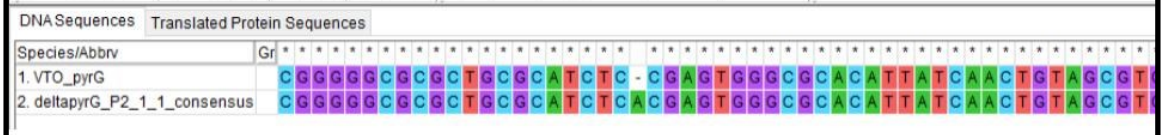

Figure 15: Sequencing Results Following Δ*pyrG* Transformation in *Aspergillus terreus* (Δ*pyrG*_2 mutant). Consensus region of forward and reverse sequencing results of the Δ*pyrG*_2 mutant guide sequence underlined, **PAM sequence** bolded, and a * denoting the expected cut site after a classical CRISPR event. Orange A base is an insertion inconsistent with wild-type 5 bp upstream of PAM site. ClustalW alignment of VTO and mutant sequences over the affected region denoting insertion as a - character in the VTO sequence

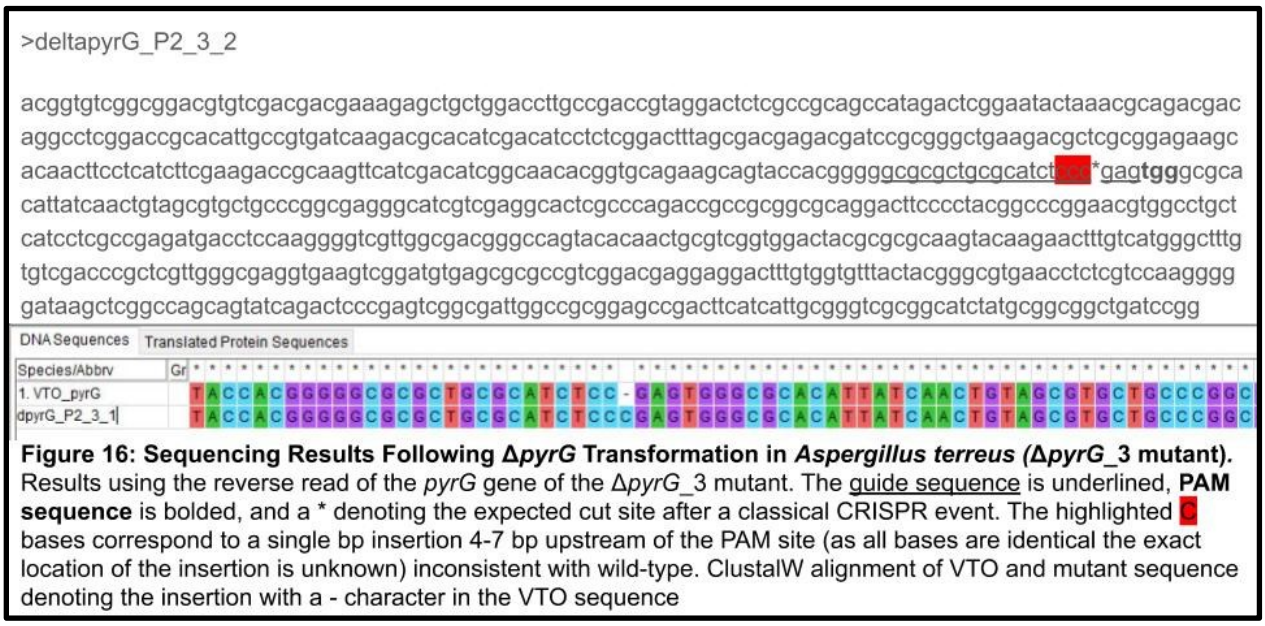

Figure 16: Sequencing Results Following Δ*pyrG* Transformation in *Aspergillus terreus* (Δ*pyrG*_3 mutant). Results using the reverse read of the *pyrG* gene of the Δ*pyrG*_3 mutant. The guide sequence is underlined, **PAM sequence** is bolded, and a * denoting the expected cut site after a classical CRISPR event. The highlighted C bases correspond to a single bp insertion 4-7 bp upstream of the PAM site (as all bases are identical the exact location of the insertion is unknown) inconsistent with wild-type. ClustalW alignment of VTO and mutant sequence denoting the insertion with a - character in the VTO sequence

Investigation of Plasmid Extrachromosomality

After the Δ*pyrG* genotype and phenotype were confirmed in the selection strain, it was investigated for full removal of the ANEp8-*amds-cas9*(Δ*pyrG)* plasmid via comparison of the strain to wild type on various selective media. The purpose of this investigation is to determine if the plasmid retains its ability to function without incorporation into the genome, thereby allowing a smaller genomic footprint for alterations. Additionally, lack of evidence for plasmid integration would support the hypothesis that genes are disrupted through CRISPR events instead of random plasmid integration. This was completed by assaying the mutant strain by growing it on various selective media for the presence of phenotypical characteristics that would indicate whether the acetamidase selection marker used on the plasmid is still present or absent. After five days growth on SRM, NSRM, NSRM + acetamide, NSRM + fluoro-acetamide, and NSRM + 5-FOA, the results were as shown in Figure 17. On SRM the wild-type shows good growth, and the Δ*pyrG* strain shows no growth, confirming a lack of functional endogenous uridine/uracil synthesis. On NSRM both wild-type and the Δ*pyrG* strain demonstrate good growth, consistent with there being no selection pressure present. On NSRM + acetamide both strains show poor growth consistent with

a lack of nitrogen and indicating that neither strain has a functional acetamidase gene present. This indicates successful removal of the plasmid from the Δ*pyrG* selection strain, post-transformation. On NSRM + fluoro-acetamide both wild-type and the Δ*pyrG* strain show poor growth consistent with a lack of nitrogen. Furthermore, neither strain shows the strong growth inhibition that would be expected following metabolism of fluoro-acetamide, indicating that neither strain has a functional acetamidase gene present. Finally, on NSRM + 5-FOA the Δ*pyrG* strain shows no reduced growth, and the wild-type strain shows no growth, indicating greater susceptibility of the wild-type to 5-FOA induced metabolic poisoning. This is consistent with the presence of a functional *pyrG* gene in the wild-type.

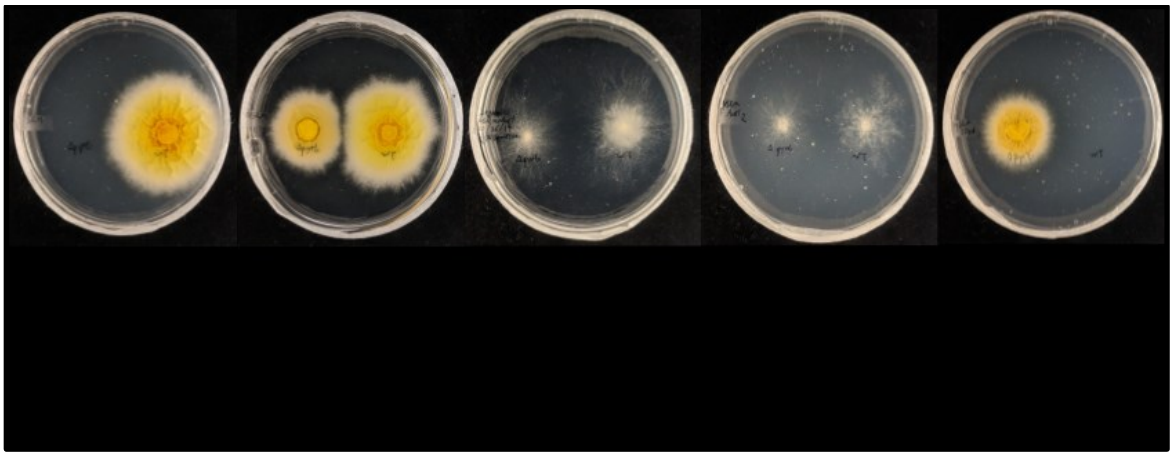

Screening and Isolation of *ΔmelA* Mutants: Throughout the experiments described to this point, the observed frequency of knockout mutants was very low. To investigate the frequency of knockout mutants more quickly, strains were constructed with an easily identifiable visual phenotype. The *melA* gene is responsible for the wild-type “cinnamon brown” coloration of *A. terreus* spores. Inactivation of this gene leads to albino colonies that can be easily identified and tallied by visual inspection. To simplify analysis, experiments were performed with a single plasmid designed and assembled as above (see *Methods*). Following transformation with the plasmid transformants were grown for ~5 days until conidial pigmentation was strong and apparent. Then those with a *melA* deletion were identified by visual identification of colonies producing white spores. Following two rounds of re-plating and isolation only one stable albino mutant was

isolated from the 76 initially observed transformants, corresponding to a knockout frequency of 1.3%. For the subsequent transformation of this strain with different concentrations of DNA this frequency roughly held true over all the colonies with 10 colonies of 936 (1.06%) showing the albino phenotype. These mutants however did display a phenotype characteristic of *A. terreus* whose only observed variation was that the wild-type brown colored spores were instead white, with a full plate of white colonies obtained after isolation and replating (Figure 18). This indicates that while several protoplasts were able to express the plasmid a vast majority did not experience inactivation of the targeted gene. Sanger sequencing of one of the albino mutants indicated a CRISPR-consistent mutation within the *melA* gene of a single bp deletion 4 bases upstream of the PAM sequence (Figure 19, for specific primers used see Table S1).

Figure 18: Comparison of Wild-type and Prospective Δ*melA A. terreus*. Wild-type (left) and one prospective Δ*melA* (right) *A. terreus* after 4 days growth at 37°C on NSRM

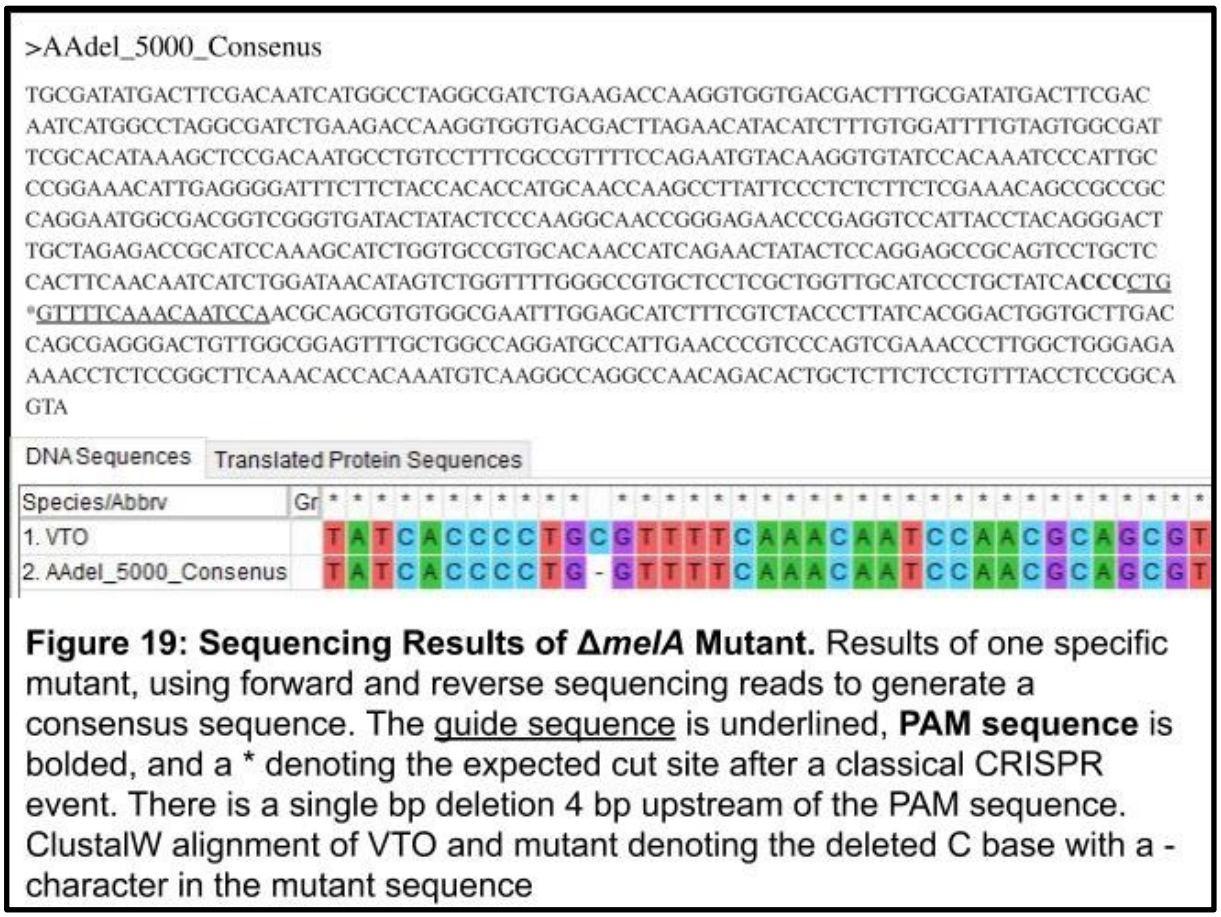

Figure 19: Sequencing Results of Δ*melA* Mutant. Results of one specific mutant, using forward and reverse sequencing reads to generate a consensus sequence. The guide sequence is underlined, **PAM sequence** is bolded, and a * denoting the expected cut site after a classical CRISPR event. There is a single bp deletion 4 bp upstream of the PAM sequence. ClustalW alignment of VTO and mutant denoting the deleted C base with a - character in the mutant sequence

Knockout Investigations for Improving Itaconic Acid Production

With an effective *A. terreus* transformation procedure worked out, two different host *A. terreus* strains generated, and the feasibility of using CRISPR-Cas9 in *A. terreus* demonstrated, it became possible to target genes of interest that may be involved in improving itaconic acid production for deletion.

Plasmid Assembly: All designed guides (see ”CRISPR-Cas9 Guide Identification”) were successfully assembled via fusion PCR and the appropriate size was verified via gel electrophoresis, followed by introduction into the ANEp8-*pyrG-cas9*-LIC2 vector, as described in *Methods* (Figure 3).

E. coli Transformation: Following transformation of all assembled plasmids (ANEp8-*amdS-cas9* [Δ*pyrg*] or ANEp8-*pyrG-cas9*[various guides]) into *E.coli*, two ampicillin-

resistant colonies were selected from each transformation plate for colony PCR screening for inserts of the correct size. For the three *A. niger* ortholog target genes chosen, at least one positive was identified from each transformation for each of the two plasmids generated per gene (i.e. six positive plasmids in total). Primers for colony PCR flanked the insert regions on the plasmid, therefore the procedure includes an internal control wherein empty vectors can be identified by a 131bp band and a fully assembled plasmid results in a 490bp fragment (as shown in Figure 4). All plasmids except plasmid five (lanes 6 and 15) displayed at least one positive result (Figure 20)

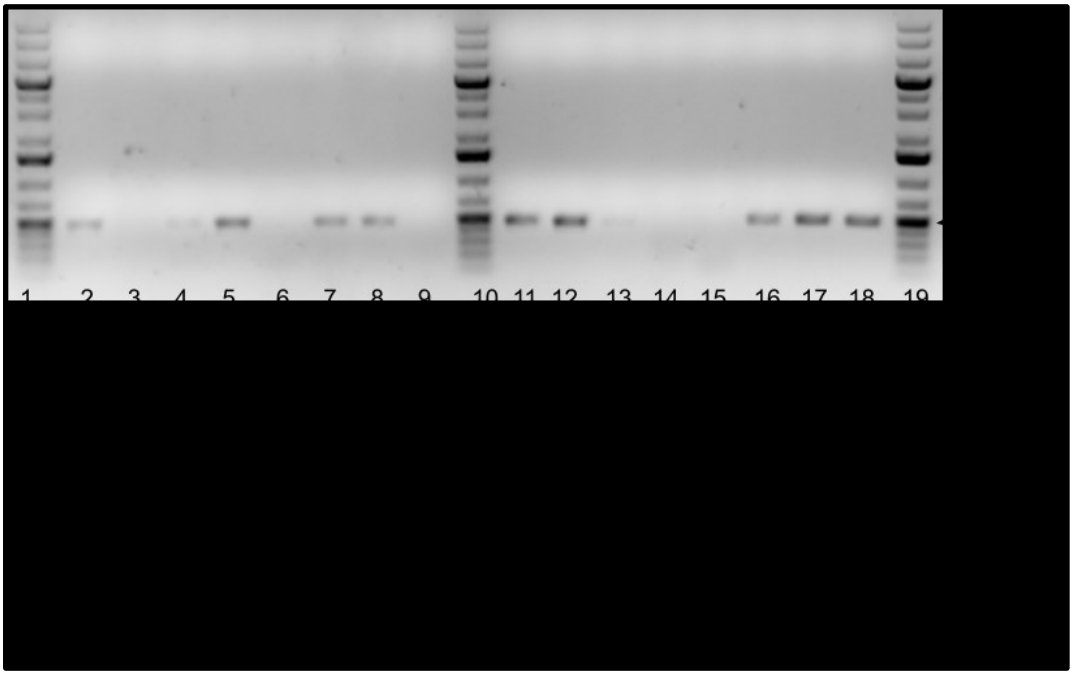

Restriction Digest Verification of LIC-Assembled Plasmids: All colony PCR-identified plasmids were re-verified for the correct inserts using two separate restriction enzyme digests (see *Methods*). Fragments observed for all plasmids were of expected sizes after EcoRI digestion. The presence of an insert was also verified for each plasmid by SmaI digestion: there are two SmaI cut sites in the parent LIC plasmid, and three cut sites in a plasmid which has had an insert introduced at the LIC site (see Figure 8).

Construction of Target Gene Deletion Strains in *A. terreus*: Transformation of *A. terreus* NRRL 1960 Δ*pyrG* with the ANEp8-*pyrG-cas9* plasmids, two each for the deletion of the

orthologs of the *A. niger* genes (two plasmids plus repair template for each), generated 63, 125, and 104 colonies when plated on NSRM, respectively. Transformation efficiencies for the control, ortholog A, ortholog B, and ortholog C were 96, 57.3, 69.4, and 94.5 transformants per µg of plasmid DNA, respectively.

Table 5: *Aspergillus niger* Ortholog Deletions in *Aspergillus terreus* Transformation

Target	Transformation Efficiency (transformants/ µg)
None (Control)	96
Ortholog A	57.3
Ortholog B	69.4
Ortholog C	94.5

Screening of Potential Knockout Transformants: Colonies were selected from the previous step (10 for each gene, and a vector-only control) for initial screening of deletions of the orthologs of the *A. niger* genes. Two colonies from each experimental condition showed integration of the homology-directed repair template as determined via PCR analysis of extracted genomic DNA using the upstream forward and downstream reverse primers used to assemble the homology-directed repair template (Figure 5 and 21 [Lanes 12 and 13]). This amplification pattern remained constant over several rounds of screening: as the repair template contains no selection marker this indicates genomic integration of the repair template. However, further screening using primers specific to regions of the wild-type gene that should have been removed following the planned deletion showed products of identical size to the wild-type strain (Figure 22 [Lanes 2 and 3]). This observation holds true for all transformants screened. In short, the colonies were screened with the upstream forward and downstream reverse primers used to construct the HDRTs (Figure 5), which should have a product

size of 1727 bp if the HDRT was successfully incorporated, leading to a deletion, or 2589 bp if the HDRT was not incorporated and the entire gene was therefore present. While 20% of screened mutants showed this pattern (Figure 21), when the mutants which seemed to display a knockout genotype were re-screened with primers designed to amplify a region which should have been removed, a product of the wildtype size was still observed (Figure 22). This observation is consistent with ectopic integration of the repair template, not integration at the site of the wild-type gene following a CRISPR-Cas9 double-stranded DNA break: this surprising result will be examined below in the *Discussion*.

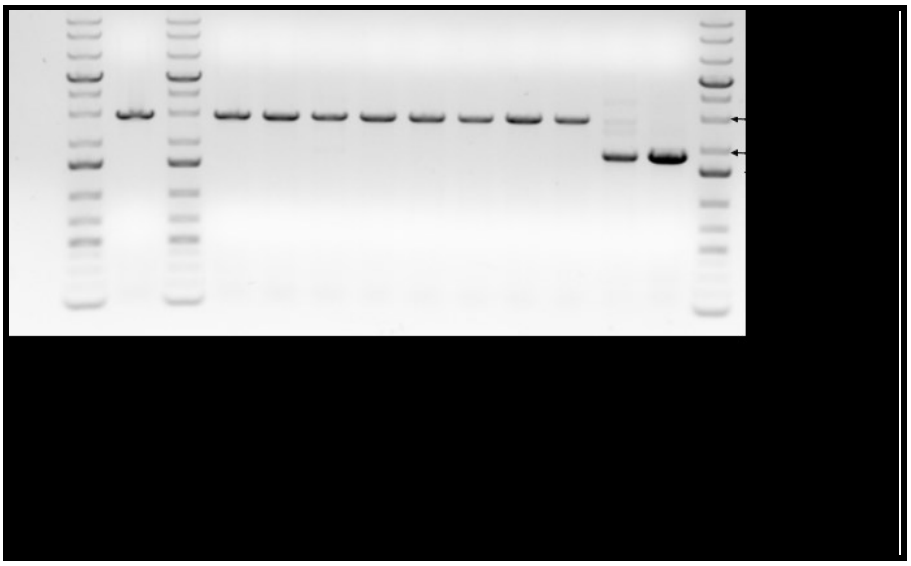

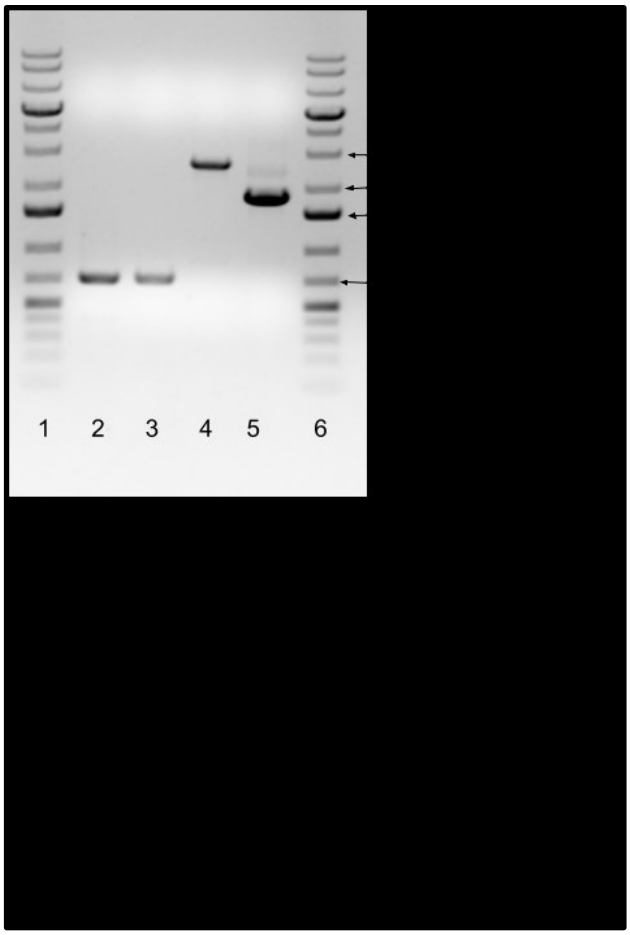
1
2
3
4
5
6

Discussion

This thesis describes the first successful use of CRISPR-Cas9 in the industrial organic acid producer, *Aspergillus terreus*. A scaffold assembly of the genome of the previously-unsequenced NRRL1960 strain of *A. terreus* was generated and used to construct recombinant extrachromosomal plasmids for CRISPR-Cas9 applications. These plasmids were successfully transformed into *A. terreus* strain 1960 leading to the creation of several stable strains that can be used for the selection of genetic markers introduced in association with genome-targeted gene deletion or augmentation. One of these strains is a *pyrG* deletion, which has exhibited stable uridine and uracil auxotrophy over several generations. However, despite this success with CRISPR-Cas9, two limitations were that the observed frequency of gene disruptions was quite low in the absence of a strong selection marker for the deletion itself, and no integration of repair templates was observed.

The results reported here are based on adaptation of the ANEp8 system, developed originally for *A. niger*, to introduce precise CRISPR-Cas9-based edits in *A. terreus*. Stable mutants that serve as transformation and selection strains were generated. For the transformations themselves, the predicted phenotypes were observed, as expected based on the previous literature regarding gene function [68]. In *A. terreus* successful ANEp8-*amdS*-*cas9*(Δ*pyrG*) transformations showed efficiencies up to 46 colonies per µg plasmid DNA with an average efficiency of 9.90 transformants per µg (standard deviation 13.1) demonstrating that this organism was transformed less effectively than others in the genus[66]. However, alterations were able to increase the average efficiency up to 114.5 transformants per µg (standard deviation 57.03). So while variation is still high, significant improvements were achieved. This is, howewer, markedly lower than the 148 colonies per µg reported in *A. niger* for this system [66]. This may be a result of reduced efficacy of the plasmid itself, which was designed for *A. niger* and utilizes *A. nidulans* genetic elements, in *A. terreus* which is a more distant relative of these two species.

Specifically, the results of the transformation of the ANEp8-*amds-cas9*(Δ*pyrG*) plasmid into *A. terreus* NRRL1960 demonstrated that the system can effectively inactivate genes in *A. terreus* as hypothesized (see Figure 10). Closer analysis indicated all mutations observed were consistent with CRISPR-Cas9 and that all alterations came about as a result of Cas9 nuclease activity as planned (See Figures 12, 15, and 16) [66]. Further investigations also demonstrated that not only was this process reversible through transformation with a plasmid containing an active copy of the inactivated gene (See Figure 11), but that no vestigial activity of the acetamidase selection marker was found (See Figure 17). This indicates that the selection marker can be reconstituted to regenerate a phenotype similar to that of the wildtype, so that selection markers can be recycled for future use.

Similarly, the results of the transformation using the ANEp8-*pyrG-cas9*(*ΔmelA*) plasmid indicate that CRISPR-Cas9-based deletions can be carried out even without a form of selection for the mutant phenotype. Analysis of the genotype of one of the isolated mutants agrees with the conclusions of the above experiments and supports the hypothesis that this system can be used to introduce small CRISPR-Cas9-consistent gene alterations (See Figure 18). In contrast to the *pyrG* experiments, this experiment has the advantage that the rate of gene inactivation can be quantitated, and it was lower than expected at ~1%. As there has never been an investigation of CRISPR-Cas9 in *A. terreus* it is impossible to compare directly, however it is at the low end of the range reported for the genus (1-100%)[61] and significantly lower than the 12.28% previously reported for wildtype *A. niger* using this system [66]. This would suggest a reduced response of this organism to the system that might be improved with additional adjustments to the protocol.

The attempted deletion of the three *A. niger* orthologs believed to be related to citric acid production proved to be the least tractable part of this study. While the analysis of the transformants showed a 20% rate of incorporation of the repair template (Figure 21), which was in line with expectations, closer analysis indicated that the repair template was not incorporated at the desired locus (Figure 22). Rather all repair templates were integrated at random sites in the genome (Figure 22) in contrast to the

observations of Couch and Gaucher (2003) wherein half of observed mutants had integration at the expected site, although this investigation utilized circular repair templates [84]. This is problematic as the experimental design was intended to allow incorporation of these templates to cause large predictable deletions. This result also contrasts with the observations of Nødvig et al. (2018) who, in *A. niger*, observed an incorporation rate close to 100% with an almost identical approach but, notably, in an NHEJ-deficient strain [63]. While the apparent inability of *A. terreus* to incorporate DNA is not consistent with other CRISPR-Cas9 investigations in *Aspergilli,* it is likely just a result of the observed low efficiency of this system in causing CRISPR-Cas9 cuts and not a result of any species-specific characteristic. The influence of the NHEJ deficiency will be explored further below.

The results of this investigation are overall in line with previous investigations and literature. The first description of CRISPR-Cas9 in the *Aspergillus* genus demonstrated that this system could be used to alter the genomes of other organisms in the genus [62]. However, until now the industrially valuable *A. terreus* has not been altered using CRISPR-Cas9. This is despite several publications detailing gaps in current knowledge that could be addressed through the generation of additional knockout strains [3]. This investigation has extended the use of CRISPR-Cas9 to this important fungus and opened the opportunity for the creation of additional strains. Significantly, it has shown that stable knockout mutants can be constructed using similar methods as previously applied to other organisms within this genus. While knockout methods have been utilized previously in *A. terreus* these methods were based on homologous recombination and therefore required the construction of very large homology flanks and necessitated the integration of a limited number of selection markers [67]. The system demonstrated in this investigation has the potential for very small (less than 100 bp, usually less than 2 bp) alterations and theoretically endless capacity for iterative recycling of selection markers. This gives this system a significant advantage in that there is no theoretical maximum in the number of genes that can be deactivated within a single strain allowing for more advanced strain engineering and analysis of gene interactions between a greater number of genes.

Additionally, some of the unexpected limitations of the approach in this organism as opposed to others has been revealed. Predominantly, this investigation was unable to achieve the inactivation rates observed in other *Aspergilli* and precise integration of repair templates at the cut site was also not obtained. Therefore, while the system can be used to generate knockout mutants, additional work will be necessary to create precise insertions and exact large knockouts.

Overall, the observed limitations in the system that has been investigated are likely dependent on a combination of factors. In particular, the observed frequency of the stable albinos in the Δ*melA* transformation is, as described above, at the very bottom of the range reported for other Aspergilli. This serves as a clear indication that the system in use is not very efficient in *A. terreus* in the absence of strong selection favoring the knockout. Therefore, optimization of the plasmid system itself, via codon optimization and the use of strong constitutive *A. terreus* promoters, would likely increase the utility of CRISPR-Cas9 in *A. terreus*. Furthermore, as NHEJ is likely the dominant repair mechanism in *A. terreus,* and deletion of this mechanism has shown vast improvements in both efficiency and accuracy of CRISPR-Cas9 editing in other filamentous fungi[66], its disruption in *A. terreus* would likely be a strategy that would lead to an improvement in observed outcomes.

Conclusions and Future Work

Overall, this investigation resulted in the construction of an effective uridine/uracil auxotroph that serves as a stable selection strain. The nature and location of the observed disruptive mutation are consistent with a Cas9 mechanism[3]. However, even with this strain in hand no precise deletions using incorporation of a repair template were observed (Figure 22). As a result, engineering of an improved itaconic acid producing phenotype based on knockout of the *A. niger* orthologs was not possible at this point. Furthermore, this inability to induce specific mutations and the low observed frequency of Cas9-based disruptions in *A. terreus* indicates that in its current form this system is not a significant improvement over previously-described methods such as homologous recombination for this species. However, based on the results obtained here, several steps could be taken which would likely yield increased transformation efficiencies and repair template integration either by improving the system or further engineering the fungus itself to be more tractable in terms of genetic manipulation.

For the improvement of the CRISPR-Cas9 system in *A. terreus* NRRL1960, the first substantial step would be the annotation of the scaffold assembly. Once the contig assembly is organized into a “genome” transcriptomic analysis would become much easier and more accurate. This would allow for both the identification of strong promoters for use in plasmid systems (such as to drive endogenous expression of *cas9*) and would also allow for analysis of *A. terreus* NRRL1960’s codon usage patterns. The codon optimization of the ANEp8 plasmids could then be compared to the genomic codon usage of *A. terreus* to see if there are significant variations. The plasmid could then be re-optimized for *A. terreus* and put under the control of strong endogenous promoters. Expression of *cas9* using this system could then be evaluated using a reporter system such as GFP [85].

If these changes prove insufficient to generate a fully functional gene-editing system further improvements could likely be achieved by deleting the genes responsible for the NHEJ pathway in *A. terreus* [62]. While the resultant strain may have

characteristics, such as increased susceptibility to mechanical and oxidative stress[86], that are detrimental to use as an industrial producer of itaconic acid the deleted genes could be reconstituted once the desired genetic alterations have been carried out. The deletion of the genes responsible (kus70 and/or kus80) could either be attempted using CRISPR-Cas9 or simply performed using homologous recombination [68]. By compromising NHEJ a strong pressure is applied that favors the organism's utilization of supplied templates to Cas9-induced double-stranded DNA breaks because otherwise it has a severely compromised ability to repair these breaks leading to significant lethality[86,87].

With a NHEJ deficient strain in hand any obstacles presented by the potential multinuclear or heterokaryotic nature of *A. terreus* could be overcome through experimental design by employing a selection marker on the *cas9* plasmid and a different selection marker on the repair template. Simultaneously selecting for both markers should lead to very high-throughput transformations as the plasmid selection marker will guarantee the presence of the *cas9* plasmid, and the repair template selection will force the organism to either repair any induced double-stranded breaks with the template or lead to high lethality in the organism. While this would likely increase the efficiency and accuracy of transformation it would however require the use of a separate selection marker for each desired deletion, one of the major drawbacks of already available methods.

Any of these adaptations would likely lead to an improvement in the observed efficacy of CRISPR-Cas9 in *A. terreus*, but as there are no published investigations of its utilization in this fungus it is impossible to know for sure. Given the fact that no other organism has yet been shown to achieve titers of itaconic acid on par with *A. terreus*[6], if continuing trends towards a greener bioeconomy continue this may likely change.

References

(1) Werpy, T.; Petersen, G. *Top Value Added Chemicals from Biomass: Volume I -- Results of Screening for Potential Candidates from Sugars and Synthesis Gas*; DOE/GO-102004-1992, 15008859; 2004.

(2) Lai, L.-S. T.; Hung, C.-S.; Lo, C.-C. Effects of Lactose and Glucose on Production of Itaconic Acid and Lovastatin by *Aspergillus Terreus* ATCC 20542. *J. Biosci. Bioeng.* **2007**, *104* (1), 9–13.

(3) Karaffa, L.; Kubicek, C. P. Citric Acid and Itaconic Acid Accumulation: Variations of the Same Story? *Appl. Microbiol. Biotechnol.* **2019**, *103* (7), 2889–2902. https://doi.org/10.1007/s00253-018-09607-9.

(4) Chen, Y.; Nielsen, J. Biobased Organic Acids Production by Metabolically Engineered Microorganisms. *Curr. Opin. Biotechnol.* **2016**, *37*, 165–172. https://doi.org/10.1016/j.copbio.2015.11.004.

(5) Willke, T.; Vorlop, K. D. Biotechnological Production of Itaconic Acid. *Appl. Microbiol. Biotechnol.* **2001**, *56* (3–4), 289–295.

(6) Kuenz, A.; Krull, S. Biotechnological Production of Itaconic Acid—Things You Have to Know. *Appl. Microbiol. Biotechnol.* **2018**, *102* (9), 3901–3914. https://doi.org/10.1007/s00253-018-8895-7.

(7) Bafana, R.; Pandey, R. A. New Approaches for Itaconic Acid Production: Bottlenecks and Possible Remedies. *Crit. Rev. Biotechnol.* **2018**, *38* (1), 68–82.

(8) Saha, B. C. Emerging Biotechnologies for Production of Itaconic Acid and Its Applications as a Platform Chemical. *J. Ind. Microbiol. Biotechnol.* **2017**, *44* (2), 303–315. https://doi.org/10.1007/s10295-016-1878-8.

(9) Klement, T.; Büchs, J. Itaconic Acid–a Biotechnological Process in Change. *Bioresour. Technol.* **2013**, *135*, 422–431.

(10) Karaffa, L.; Díaz, R.; Papp, B.; Fekete, E.; Sándor, E.; Kubicek, C. P. A Deficiency of Manganese Ions in the Presence of High Sugar Concentrations Is the Critical Parameter for Achieving High Yields of Itaconic Acid by *Aspergillus Terreus*. *Appl. Microbiol. Biotechnol.* **2015**, *99* (19), 7937–7944. https://doi.org/10.1007/s00253-

015-6735-6.

(11) Lin, M. M. Selective Oxidation of Propane to Acrylic Acid with Molecular Oxygen. *Appl. Catal. Gen.* **2001**, *207* (1–2), 1–16. https://doi.org/10.1016/S0926-860X(00)00609-8.

(12) Baup, S. Ueber Eine Neue Pyrogen-Citronensäure Und Über Benennung Der Pyrogen-Säuren Überhaupt. *Ann Chim Phys* **1837**, *19*, 29–38.

(13) Cordes, T.; Michelucci, A.; Hiller, K. Itaconic Acid: The Surprising Role of an Industrial Compound as a Mammalian Antimicrobial Metabolite. *Annu. Rev. Nutr.* **2015**, *35*, 451–473. https://doi.org/10.1146/annurev-nutr-071714-034243.

(14) Cavallo, E.; Charreau, H.; Cerrutti, P.; Foresti, M. L. *Yarrowia Lipolytica*: A Model Yeast for Citric Acid Production. *FEMS Yeast Res.* **2017**, *17* (8). https://doi.org/10.1093/femsyr/fox084.

(15) Hou, W.; Bao, J. Simultaneous Saccharification and Aerobic Fermentation of High Titer Cellulosic Citric Acid by Filamentous Fungus *Aspergillus Niger*. *Bioresour. Technol.* **2018**, *253*, 72–78. https://doi.org/10.1016/j.biortech.2018.01.011.

(16) Kinoshita, K. Über Die Produktion von Itaconsäure Und Mannit Durch Einen Neuen Schimmelpilz *Aspergillus Itaconicus*. *Acta Phytochim.* **1932**, *5*, 271–287.

(17) Calam, C. T.; Oxford, A. E.; Raistrick, H. Studies in the Biochemistry of Micro-Organisms: Itaconic Acid, a Metabolic Product of a Strain of *Aspergillus Terreus* Thom. *Biochem. J.* **1939**, *33* (9).

(18) Li, P.; Ma, S.; Dai, J.; Liu, X.; Jiang, Y.; Wang, S.; Wei, J.; Chen, J.; Zhu, J. Itaconic Acid as a Green Alternative to Acrylic Acid for Producing a Soybean Oil-Based Thermoset: Synthesis and Properties. *ACS Sustain. Chem. Eng.* **2017**, *5* (1), 1228–1236. https://doi.org/10.1021/acssuschemeng.6b02654.

(19) Blazeck, J.; Miller, J.; Pan, A.; Gengler, J.; Holden, C.; Jamoussi, M.; Alper, H. S. Metabolic Engineering of *Saccharomyces Cerevisiae* for Itaconic Acid Production. *Appl. Microbiol. Biotechnol.* **2014**, *98* (19), 8155–8164. https://doi.org/10.1007/s00253-014-5895-0.

(20) Huang, X.; Lu, X.; Li, Y.; Li, X.; Li, J.-J. Improving Itaconic Acid Production through Genetic Engineering of an Industrial *Aspergillus Terreus* Strain. *Microb. Cell Factories* **2014**, *13* (1).

(21) Saha, B. C.; Kennedy, G. J.; Bowman, M. J.; Qureshi, N.; Dunn, R. O. Factors Affecting Production of Itaconic Acid from Mixed Sugars by *Aspergillus Terreus*. *Appl. Biochem. Biotechnol.* **2019**, *187* (2), 449–460. https://doi.org/10.1007/s12010-018-2831-2.

(22) Medway, A. M.; Sperry, J. Heterocycle Construction Using the Biomass-Derived Building Block Itaconic Acid. *Green Chem* **2014**, *16* (4), 2084–2101. https://doi.org/10.1039/C4GC00014E.

(23) Arabatzis, M.; Velegraki, A. Sexual Reproduction in the Opportunistic Human Pathogen *Aspergillus Terreus*. *Mycologia* **2013**, *105* (1), 71–79. https://doi.org/10.3852/11-426.

(24) Balajee, S. A.; Houbraken, J.; Verweij, P. E.; Hong, S.-B.; Yaghuchi, T.; Varga, J.; Samson, R. A. Aspergillus Species Identification in the Clinical Setting. *Stud. Mycol.* **2007**, *59*, 39–46. https://doi.org/10.3114/sim.2007.59.05.

(25) Thom, C.; Church, M. B. *Aspergillus Fumigatus, A. Nidulans, A. Terreus* N. Sp. and Their Allies. *Am. J. Bot.* **1918**, *5* (2). https://doi.org/10.2307/2435130.

(26) Jahromi, M. F.; Liang, J. B.; Ho, Y. W.; Mohamad, R.; Goh, Y. M.; Shokryazdan, P. Lovastatin Production by *Aspergillus Terreus* Using Agro-Biomass as Substrate in Solid State Fermentation. *J. Biomed. Biotechnol.* **2012**, *2012*. https://doi.org/10.1155/2012/196264.

(27) Slejko, J. F.; Basu, A.; Sullivan, S. D. Returns to Scientific Publications for Pharmaceutical Products in the United States. *Health Econ.* **2018**, *27* (2), 282–293. https://doi.org/10.1002/hec.3546.

(28) Li, A.; van Luijk, N.; Ter Beek, M.; Caspers, M.; Punt, P.; van der Werf, M. A Clone-Based Transcriptomics Approach for the Identification of Genes Relevant for Itaconic Acid Production in Aspergillus. *Fungal Genet. Biol.* **2011**, *48* (6), 602–611.

(29) Krull, S.; Hevekerl, A.; Kuenz, A.; Prüße, U. Process Development of Itaconic Acid Production by a Natural Wild Type Strain of *Aspergillus Terreus* to Reach Industrially Relevant Final Titers. *Appl. Microbiol. Biotechnol.* **2017**, *101* (10), 4063–4072.

(30) Yahiro, K.; Takahama, T.; Park, Y. S.; Okabe, M. Breeding of *Aspergillus Terreus*

Mutant TN-484 for Itaconic Acid Production with High Yield. *J. Ferment. Bioeng.* **1995**, *79* (5), 506–508. https://doi.org/10.1016/0922-338X(95)91272-7.

(31) Reddy, C. S. K.; Singh, R. P. Enhanced Production of Itaconic Acid from Corn Starch and Market Refuse Fruits by Genetically Manipulated *Aspergillus Terreus* SKR10. *Bioresour. Technol.* **2002**, *85* (1), 69–71. https://doi.org/10.1016/S0960-8524(02)00075-5.

(32) Shin, W.-S.; Park, B.; Lee, D.; Oh, M.-K.; Chun, G.-T.; Kim, S. Enhanced Production of Itaconic Acid through Development of Transformed Fungal Strains of *Aspergillus Terreus*. *J. Microbiol. Biotechnol.* **2017**, *27* (2), 306–315.

(33) Chen, M.; Huang, X.; Zhong, C.; Li, J.; Lu, X. Identification of an Itaconic Acid Degrading Pathway in Itaconic Acid Producing *Aspergillus Terreu*s. *Appl. Microbiol. Biotechnol.* **2016**, *100* (17), 7541–7548.

(34) Vuoristo, K. S.; Mars, A. E.; Sangra, J. V.; Springer, J.; Eggink, G.; Sanders, J. P. M.; Weusthuis, R. A. Metabolic Engineering of Itaconate Production in *Escherichia Coli*. *Appl. Microbiol. Biotechnol.* **2015**, *99* (1), 221–228. https://doi.org/10.1007/s00253-014-6092-x.

(35) Steiger, M. G.; Blumhoff, M. L.; Mattanovich, D.; Sauer, M. Biochemistry of Microbial Itaconic Acid Production. *Front. Microbiol.* **2013**, *4*.

(36) E., S.; N., D.-C.; J., F.; Dijck, P. van. On the Safety of *Aspergillus Niger* - a Review. *Appl. Microbiol. Biotechnol.* **2002**, *59* (4–5), 426–435. https://doi.org/10.1007/s00253-002-1032-6.

(37) Cairns, T. C.; Nai, C.; Meyer, V. How a Fungus Shapes Biotechnology: 100 Years of *Aspergillus Niger* Research. *Fungal Biol. Biotechnol.* **2018**, *5* (1). https://doi.org/10.1186/s40694-018-0054-5.

(38) Papagianni, M. Advances in Citric Acid Fermentation by *Aspergillus Niger*: Biochemical Aspects, Membrane Transport and Modeling. *Biotechnol. Adv.* **2007**, *25* (3), 244–263. https://doi.org/10.1016/j.biotechadv.2007.01.002.

(39) Show, P. L.; Oladele, K. O.; Siew, Q. Y.; Aziz Zakry, F. A.; Lan, J. C.-W.; Ling, T. C. Overview of Citric Acid Production from *Aspergillus Niger*. *Front. Life Sci.* **2015**, *8* (3), 271–283. https://doi.org/10.1080/21553769.2015.1033653.

(40) Steiger, M. G.; Rassinger, A.; Mattanovich, D.; Sauer, M. Engineering of the

Citrate Exporter Protein Enables High Citric Acid Production in *Aspergillus Niger*. *Metab. Eng.* **2019**, *52*, 224–231. https://doi.org/10.1016/j.ymben.2018.12.004.

(41) Krebs, H. A.; Salvin, E.; Johnson, W. A. The Formation of Citric and Alpha-Ketoglutaric Acids in the Mammalian Body. *Biochem. J.* **1938**, *32* (1), 113–117. https://doi.org/10.1042/bj0320113.

(42) Cleland, W. W.; Johnson, M. J. Tracer Experiments on the Mechanism of Citric Acid Formation by *Aspergillus Niger*. *J. Biol. Chem.* **1954**, *208* (2), 679–689.

(43) Peksel, A.; Torres, N. V.; Liu, J.; Juneau, G.; Kubicek, C. P. 13C-NMR Analysis of Glucose Metabolism during Citric Acid Production by *Aspergillus Niger*. *Appl. Microbiol. Biotechnol.* **2002**, *58* (2), 157–163.

(44) Karaffa, L.; Kubicek, C. P. *Aspergillus Niger* Citric Acid Accumulation: Do We Understand This Well Working Black Box? *Appl. Microbiol. Biotechnol.* **2003**, *61* (3), 189–196.

(45) Kirimura, K.; Kobayashi, K.; Ueda, Y.; Hattori, T. Phenotypes of Gene Disruptants in Relation to a Putative Mitochondrial Malate–Citrate Shuttle Protein in Citric Acid-Producing *Aspergillus Niger*. *Biosci. Biotechnol. Biochem.* **2016**, *80* (9), 1737–1746. https://doi.org/10.1080/09168451.2016.1164583.

(46) Tong, Z.; Zheng, X.; Tong, Y.; Shi, Y.-C.; Sun, J. Systems Metabolic Engineering for Citric Acid Production by *Aspergillus Niger* in the Post-Genomic Era. *Microb. Cell Factories* **2019**, *18* (1). https://doi.org/10.1186/s12934-019-1064-6.

(47) Tsao, G. T.; Cao, N. J.; Du, J.; Gong, C. S. Production of Multifunctional Organic Acids from Renewable Resources. *Adv. Biochem. Eng. Biotechnol.* **1999**, *65*, 243–280.

(48) Perlman, D. Physiological Studies on the Actinomycetes. *Bot. Rev.* **1953**, *19* (1), 46–97. https://doi.org/10.1007/BF02861726.

(49) Gardner, J. F.; James, L. V.; Rubbo, S. D. Production of Citric Acid by Mutants of *Aspergillus Niger*. *J. Gen. Microbiol.* **1956**, *14* (2), 228–237. https://doi.org/10.1099/00221287-14-2-228.

(50) Trumpy, B. H.; Millis, N. F. Nutritional Requirements of an *Aspergillus Niger* Mutant for Citric Acid Production. *J. Gen. Microbiol.* **1963**, *30* (3), 381–393. https://doi.org/10.1099/00221287-30-3-381.

(51) Goosen, T.; Bloemheuvel, G.; Gysler, C.; de Bie, D. A.; van den Broek, H. W. J.; Swart, K. Transformation of *Aspergillus Niger* Using the Homologous Orotidine-5′-Phosphate-Decarboxylase Gene. *Curr. Genet.* **1987**, *11* (6–7), 499–503. https://doi.org/10.1007/BF00384612.

(52) Oliver, R. P.; Roberts, I. N.; Harling, R.; Kenyon, L.; Punt, P. J.; Dingemanse, M. A.; van den Hondel, C. A. M. J. J. Transformation of *Fulvia Fulva*, a Fungal Pathogen of Tomato, to Hygromycin B Resistance. *Curr. Genet.* **1987**, *12* (3), 231–233. https://doi.org/10.1007/BF00436885.

(53) Buxton, F. P.; Gwynne, D. I.; Davies, R. W. Transformation of *Aspergillus Niger* Using the *ArgB* Gene of *Aspergillus Nidulans*. *Gene* **1985**, *37* (1), 207–214.

(54) Galagan, J. E.; Calvo, S. E.; Borkovich, K. A.; Selker, E. U.; Read, N. D.; Jaffe, D.; FitzHugh, W.; Ma, L.-J.; Smirnov, S.; Purcell, S.; et al. The Genome Sequence of the Filamentous Fungus *Neurospora Crassa*. *Nature* **2003**, *422* (6934), 859–868. https://doi.org/10.1038/nature01554.

(55) Pel, H. J.; de Winde, J. H.; Archer, D. B.; Dyer, P. S.; Hofmann, G.; Schaap, P. J.; Turner, G.; de Vries, R. P.; Albang, R.; Albermann, K.; et al. Genome Sequencing and Analysis of the Versatile Cell Factory *Aspergillus Niger* CBS 513.88. *Nat. Biotechnol.* **2007**, *25* (2), 221–231. https://doi.org/10.1038/nbt1282.

(56) Galagan, J. E.; Calvo, S. E.; Cuomo, C.; Ma, L.-J.; Wortman, J. R.; Batzoglou, S.; Lee, S.-I.; Baştürkmen, M.; Spevak, C. C.; Clutterbuck, J.; et al. Sequencing of *Aspergillus Nidulans* and Comparative Analysis with *A. Fumigatus* and *A. Oryzae*. *Nature* **2005**, *438* (7071), 1105–1115. https://doi.org/10.1038/nature04341.

(57) Meyer, V. Genetic Engineering of Filamentous Fungi--Progress, Obstacles and Future Trends. *Biotechnol. Adv.* **2008**, *26* (2), 177–185. https://doi.org/10.1016/j.biotechadv.2007.12.001.

(58) Jiang, W.; Bikard, D.; Cox, D.; Zhang, F.; Marraffini, L. A. RNA-Guided Editing of Bacterial Genomes Using CRISPR-Cas Systems. *Nat. Biotechnol.* **2013**, *31*.

(59) Deng, H.; Gao, R.; Liao, X.; Cai, Y. CRISPR System in Filamentous Fungi: Current Achievements and Future Directions. *Gene* **2017**, *627*, 212–221.

(60) Tong, Y.; Weber, T.; Lee, S. Y. CRISPR/Cas-Based Genome Engineering in Natural Product Discovery. *Nat. Prod. Rep.* **2019**.

https://doi.org/10.1039/C8NP00089A.

(61) Shi, T.-Q.; Liu, G.-N.; Ji, R.-Y.; Shi, K.; Song, P.; Ren, L.-J.; Huang, H.; Ji, X.-J. CRISPR/Cas9-Based Genome Editing of the Filamentous Fungi: The State of the Art. *Appl. Microbiol. Biotechnol.* **2017**, *101* (20), 7435–7443. https://doi.org/10.1007/s00253-017-8497-9.

(62) Nødvig, C. S.; Nielsen, J. B.; Kogle, M. E.; Mortensen, U. H. A CRISPR-Cas9 System for Genetic Engineering of Filamentous Fungi. *PloS One* **2015**, *10* (7). https://doi.org/10.1371/journal.pone.0133085.

(63) Nødvig, C. S.; Hoof, J. B.; Kogle, M. E.; Jarczynska, Z. D.; Lehmbeck, J.; Klitgaard, D. K.; Mortensen, U. H. Efficient Oligo Nucleotide Mediated CRISPR-Cas9 Gene Editing in Aspergilli. *Fungal Genet. Biol.* **2018**.

(64) Yin, X.; Li, J.; Shin, H.-D.; Du, G.; Liu, L.; Chen, J. Metabolic Engineering in the Biotechnological Production of Organic Acids in the Tricarboxylic Acid Cycle of Microorganisms: Advances and Prospects. *Biotechnol. Adv.* **2015**, *33* (6 Pt 1), 830–841. https://doi.org/10.1016/j.biotechadv.2015.04.006.

(65) Tsang, A.; Bellemare, A.; Darmond, C.; Bakhuis, J. Genetic and Genomic Manipulations in *Aspergillus Niger*. In *Genetic Transformation Systems in Fungi, Volume 2*; van den Berg, M. A., Maruthachalam, K., Eds.; Springer International Publishing: Cham, 2015; pp 225–243. https://doi.org/10.1007/978-3-319-10503-1_20.

(66) Song, L.; Ouedraogo, J.-P.; Kolbusz, M.; Nguyen, T. T. M.; Tsang, A. Efficient Genome Editing Using TRNA Promoter-Driven CRISPR/Cas9 GRNA in *Aspergillus Niger*. *PLOS ONE* **2018**, *13* (8). https://doi.org/10.1371/journal.pone.0202868.

(67) Geib, E.; Gressler, M.; Viediernikova, I.; Hillmann, F.; Jacobsen, I. D.; Nietzsche, S.; Hertweck, C.; Brock, M. A Non-Canonical Melanin Biosynthesis Pathway Protects *Aspergillus Terreus* Conidia from Environmental Stress. *Cell Chem. Biol.* **2016**, *23* (5), 587–597. https://doi.org/10.1016/j.chembiol.2016.03.014.

(68) Guo, C.-J.; Knox, B. P.; Sanchez, J. F.; Chiang, Y.-M.; Bruno, K. S.; Wang, C. C. C. Application of an Efficient Gene Targeting System Linking Secondary Metabolites to Their Biosynthetic Genes in *Aspergillus Terreus*. *Org. Lett.* **2013**,

15 (14), 3562–3565. https://doi.org/10.1021/ol401384v.

(69) Van Hartingsveldt, W.; Mattern, I. E.; van Zeijl, C. M.; Pouwels, P. H.; van den Hondel, C. A. Development of a Homologous Transformation System for *Aspergillus Niger* Based on the PyrG Gene. *Mol. Gen. Genet. MGG* **1987**, *206* (1), 71–75.

(70) Kelly, J. M.; Hynes, M. J. Transformation of *Aspergillus Niger* by the *AmdS* Gene of *Aspergillus Nidulans*. *EMBO J.* **1985**, *4* (2), 475–479.

(71) Boeke, J. D.; Trueheart, J.; Natsoulis, G.; Fink, G. R. 5-Fluoroorotic Acid as a Selective Agent in Yeast Molecular Genetics. *Methods Enzymol.* **1987**, *154*, 164–175.

(72) Debets, A. J.; Swart, K.; Holub, E. F.; Goosen, T.; Bos, C. J. Genetic Analysis of *AmdS* Transformants of *Aspergillus Niger* and Their Use in Chromosome Mapping. *Mol. Gen. Genet. MGG* **1990**, *222* (2–3), 284–290.

(73) Bennett, J. W.; Lasure, L. L. *More Gene Manipulations in Fungi*; Elsevier Science: Oxford, 1991.

(74) Sambrook, J.; Russell, D. W. Agarose Gel Electrophoresis. *Cold Spring Harb. Protoc.* **2006**, *2006* (1), pdb.prot4020. https://doi.org/10.1101/pdb.prot4020.

(75) Adrian Tsang, N. S.-F. *SPORE COLLECTION AND INOCULATION STANDARD OPERATION PROCEDURE (SOP) CSP-002*; Version 2.0; Concordia University: Center for Structural and Functional Genomics, 2014.

(76) Adrian Tsang, N. S.-F. *PREPARATION OF GLYCEROL STOCKS STANDARD OPERATION PROCEDURE (SOP) CSP-006*; Version 2.0; Concordia University: Center for Structural and Functional Genomics, 2014.

(77) Zhang, Z.; Schwartz, S.; Wagner, L.; Miller, W. A Greedy Algorithm for Aligning DNA Sequences. *J. Comput. Biol. J. Comput. Mol. Cell Biol.* **2000**, *7* (1–2), 203–214. https://doi.org/10.1089/10665270050081478.

(78) Arnaud, M. B.; Cerqueira, G. C.; Inglis, D. O.; Skrzypek, M. S.; Binkley, J.; Chibucos, M. C.; Crabtree, J.; Howarth, C.; Orvis, J.; Shah, P.; et al. The Aspergillus Genome Database (AspGD): Recent Developments in Comprehensive Multispecies Curation, Comparative Genomics and Community Resources. *Nucleic Acids Res.* **2012**, *40* (D1), D653–D659.

https://doi.org/10.1093/nar/gkr875.

(79) Adrian Tsang, L. S. *Protocol of CRISPR Plasmid Construction*; Version 1.1; Concordia University: Center for Structural and Functional Genomics, 2017.

(80) Doench, J. G.; Hartenian, E.; Graham, D. B.; Tothova, Z.; Hegde, M.; Smith, I.; Sullender, M.; Ebert, B. L.; Xavier, R. J.; Root, D. E. Rational Design of Highly Active SgRNAs for CRISPR-Cas9-Mediated Gene Inactivation. *Nat. Biotechnol.* **2014**, *32* (12), 1262–1267. https://doi.org/10.1038/nbt.3026.

(81) New England Biolabs. High Efficiency Transformation Protocol (C2987H/C2987I).

(82) Mark Arentshorst and Vera Meyer, M. A. *PEG Mediated Transformation of A. Niger Using Protocol Wageningen*; Protocol; Wageningen: The Netherlands.

(83) Arentshorst, M.; Ram, A. F. J.; Meyer, V. Using Non-Homologous End-Joining-Deficient Strains for Functional Gene Analyses in Filamentous Fungi. In *Plant Fungal Pathogens*; Bolton, M. D., Thomma, B. P. H. J., Eds.; Humana Press: Totowa, NJ, 2012; Vol. 835, pp 133–150. https://doi.org/10.1007/978-1-61779-501-5_9.

(84) Couch, R. D.; Gaucher, G. M. Rational Elimination of *Aspergillus Terreus* Sulochrin Production. *J. Biotechnol.* **2004**, *108* (2), 171–177. https://doi.org/10.1016/j.jbiotec.2003.10.021.

(85) Malina, A.; Mills, J. R.; Cencic, R.; Yan, Y.; Fraser, J.; Schippers, L. M.; Paquet, M.; Dostie, J.; Pelletier, J. Repurposing CRISPR/Cas9 for in Situ Functional Assays. *Genes Dev.* **2013**, *27* (23), 2602–2614. https://doi.org/10.1101/gad.227132.113.

(86) Shrivastav, M.; De Haro, L. P.; Nickoloff, J. A. Regulation of DNA Double-Strand Break Repair Pathway Choice. *Cell Res.* **2007**, *18*, 134.

(87) Carvalho, N. D. S. P.; Arentshorst, M.; Jin Kwon, M.; Meyer, V.; Ram, A. F. J. Expanding the *Ku70* Toolbox for Filamentous Fungi: Establishment of Complementation Vectors and Recipient Strains for Advanced Gene Analyses. *Appl. Microbiol. Biotechnol.* **2010**, *87* (4), 1463–1473. https://doi.org/10.1007/s00253-010-2588-1.

Supplemental

Table S1: Primers Referenced in this Investigation		
Primer Name	Description	Sequence
P1	Common forward primer for construction of insert for ANEp8 plasmids, fwd primer with LIC tail binding to tRNAPro1promoter	CAACCTCCAATCCAATTTGACTCCGCCGAACGTACTG
P2	Common reverse primer for construction of insert for ANEp8 plasmids, rev primer with LIC tail binding to tRNAPro1promoterRev primer with LIC tail binding to tRNAPro1 terminator	ACTACTCTACCACTATTTGAAAAGCAAAAAAGGAAGGTACAAAAAAGC
P3 (ΔpyrG)	Reverse primer containing specific guide sequence for targeting pyrG in A. terreus (first 20 bp) as well as common overlap region for fusion PCR assembly of ANEp8 inserts	CTC GGA GAT GCG CAG CGC GCG ACG AGC TTA CTC GTT TCG
P4 (ΔpyrG)	Forward primer containing specific guide sequence for targeting pyrG in A. terreus (first 20 bp) as well as common overlap region for fusion PCR assembly of ANEp8 inserts	GCG CGC TGC GCA TCT CCG AGG TTT TAG AGC TAG AAA TAG CAA G
P3 (ΔmelA)	Reverse primer containing specific guide sequence for targeting melA in A. terreus (first 20 bp) as well as	CTGCGTTTTCAAACAATCCAGACGAGCTTACTCGTTTCG

	common overlap region for fusion PCR assembly of ANEp8 inserts	
P4 (ΔmelA)	Forward primer containing specific guide sequence for targeting melA in A. terreus (first 20 bp) as well as common overlap region for fusion PCR assembly of ANEp8 inserts	GCGAGAGCGTATGGTCCGTGGTTTTAGAGCTAGAAATAGCAAG
ANEp8_Scn_For	Common forward primer for screening of presence of inserts in ANEp8 plasmids, flanks insert site	TTTTCTCTTCCATTTACGC
ANEp8_Scn_Rev	Common reverse primer for screening of presence of inserts in ANEp8 plasmids, flanks insert site	GGGGATCATAATAGTACTAGCCA
PyrG_Plasmid_Scn_For	Forward screening primer for the presence of inserts in ANEp8 plasmids, first 25 bp of insert	CAACCTCCAATCCAATTTGACTCCG
PyrG_Plasmid_Scn_Rev_2	Reverse screening primer for the presence of a specific (ΔpyrG_2) guide sequence within an ANEp8 insert	CTCGGAGATGCGCAGCGCGC
PyrG_Plasmid_Scn_Rev_3	Reverse screening primer for the presence of a specific (ΔpyrG_3) guide sequence within an ANEp8 insert	CGGATCGTCTCGTCGCTAAA
PyrG_Scn_For	Forward primer for amplification of *A. terreus pyrG* gene for sequencing	ATGTCCTCCAAGTCTCAATTG
PyrG_Scn_Rev	Reverse primer for amplification of *A. terreus pyrG* gene for sequencing	GTTACCCCCAACCCTCTTC

melA_Scn_For	Forward primer for amplification of *A. terreus melA* gene for sequencing	CCA AGG TGG TGA CGA CTT AG
melA_Scn_Rev	Reverse primer for amplification of A. terreus melA gene for sequencing	GAC TTC GGT AGT AGG GTC TG